





Received 23 June 2021; revised 27 August 2021; accepted 28 August 2021.

Digital Object Identifier 10.1109/JMW.2021.3109244

# Orthogonal Versus Zero-Forced Beamforming in Multibeam Antenna Systems: Review and Challenges for Future Wireless Networks

YANKI ASLAN <sup>1</sup> (Member, IEEE), ANTOINE ROEDERER <sup>1</sup> (Life Fellow, IEEE),  
NELSON J. G. FONSECA <sup>2</sup> (Senior Member, IEEE), PIERO ANGELETTI <sup>3</sup> (Senior Member, IEEE),  
AND ALEXANDER YAROVY<sup>1</sup> (Fellow, IEEE)

(Invited Paper)

<sup>1</sup>Microwave Sensing, Signals, and Systems Section, Delft University of Technology, 2628 Delft, The Netherlands

<sup>2</sup>Antenna and Sub-Millimetre Waves Section, European Space Agency, 2200 Noordwijk, The Netherlands

<sup>3</sup>RF Payloads and Technology Division, European Space Agency, 2200 Noordwijk, The Netherlands

CORRESPONDING AUTHOR: Yanki Aslan (e-mail: Y.Aslan@tudelft.nl).

This work was supported by the European Space Agency (ESA) in the framework of the Open Space Innovation Program (OSIP) on the project titled "A key to 5G & 6G Flexible Space Connection: Antenna Butler-like Multiple Beam Forming" under Contract 4000131563.

---

**ABSTRACT** Orthogonality in multibeam antennas is revisited. The difference between orthogonal beamforming and zero-forced beamforming is highlighted. The intriguing relation between orthogonality, reciprocity and losses is recapitulated. Different approaches on the design of orthogonal beamforming networks and implementation of zero-forced beamforming strategies are shown with various examples from the antenna-research-oriented literature. The use of orthogonal and zero-forced beamforming is discussed from the communication system perspective with relevant studies from diverse disciplines. Some of the future research challenges and potential benefits are outlined for the next generation satellite and cellular communication applications.

**INDEX TERMS** Beamforming, interference suppression, multibeam antenna, orthogonality, wireless systems, zero-forcing.

---

## I. INTRODUCTION

Most arrays onboard multiple beam satellites so far, including Iridium, Globalstar, Iridium Next, have generated fixed/switched multiple beam footprints with several users per beam. The first example of an on-board array generating a beam per user is the Tracking and Data Relay Satellite System (TDRSS) [1]. The onboard S-band array was used, from 1983 onwards, to generate up to 20 simultaneous beams, each tracking a spacecraft. Signals received by the array elements were multiplexed and sent to the ground for beam forming. This is only possible with narrow band signals. The transmit Ka-band arrays of the SPACEWAY satellites [2] provided up to 24 simultaneous co-channel beams, hopped in well separated fixed footprints, with about 1 dB cross over gain loss.

Adaptive arrays with few beams have been initially flown onboard US military satellites such as the MILSTAR, Defense Satellite Communications System (DSCS), and their

successors Advanced Extremely High Frequency (AEHF) and Wideband Global Satcom (WGS), with more beams, capacity and features such as jammer nulling. Limited details are available on their payloads. X-band adaptive arrays have been also developed for European dual-use satellites: SkyNet, Sicral, Syracuse and SpainSat. More recently, adaptive array technologies have been transferred to Ku-band commercial satellites: e.g. SmallGEO's RedSat and Quantum receive arrays. Adaptive beam forming by precoding with generation of nulls in known jammer or co-channel user directions is applied in radar and early Long-Term Evolution (LTE) mobile communication systems, generally with one beam per array at a time. Therefore, in a multi-user scenario, most systems have proposed a multiplicity of single beam antenna arrays, each serving a different user [3]. Later, with the development of the Multi-User Multiple Input Multiple Output (MIMO) concept [4] and with the introduction of the

Massive MIMO technology [5], the discussions on forming multiple flexible simultaneous co-frequency beams from a large single array on the transmit side have increased. Many works have emerged, especially in the signal-processing community, that study the formation of multiple beams sharing the same time-frequency-code resources with channel state information based precoding methods for interference management [6], [7].

From the design point of view, a recent and very comprehensive review on multiple beam arrays [8] reports various developments of truly multiple beam arrays including fully-digital, fully-analog and hybrid implementations commonly seen in applications such as radio astronomy [9], military radar [10], satellite communications [11], [12], personnel imaging [13], automotive radar [14], mobile communications [15], [16] and so on. Among these options, fully-digital schemes provide the most flexible, versatile and robust performance. However, they suffer from high complexity, power consumption and cost. Analog beamforming, and in particular, beamforming networks are an attractive solution to introduce multiple beam capability in low cost mass market products [17]. On the other hand, several hybrid beamforming strategies have recently been proposed in 5G as an appealing compromise, especially at the mm-wave bands [18], [19]. It is believed that different technologies will find their applications in different contexts [20], e.g. phased arrays in base stations where the power supply is not a major problem, and beamforming networks in user terminals or drones etc., which are battery driven and thus more constrained in power consumption.

So far, most commercial space communication systems use fixed or hopped multiple beams with limited co-channel interference control. However, it can be seen in the latest state-of-the-art that phased arrays are being considered for civilian satellite applications as well. For example, Starlink space segment is using phased array antennas [21], which is also the solution under development for O3b's mPower. Similarly, with the advent of 5G/6G and allocation of frequencies in the mm-wave range for more bandwidth, modern developments of phased array solutions have emerged in the terrestrial networks. Some state-of-the-art base station antenna examples include the active integrated arrays designed by Ericsson [22], UCSD [23], IBM [24], Nokia [25], NXP [26] and Qualcomm [27], which can all generate only a single beam at a time. The industrial high-volume mm-wave 5G market is still far from true multibeam antennas due to many practical factors such as cost, design complexity, cooling and computational burden. Although there are several examples of chip-scale hybrid/digital beamforming mm-wave receivers with relatively small number of elements and concurrent beams [28]–[30], only very few practical developments of large-scale (i.e.  $> 64$ -element) truly multiple flexible beam arrays (in the form of digital beamforming [31], [32] and hybrid beamforming [33], [34]) were reported for mm-wave cellular communications.

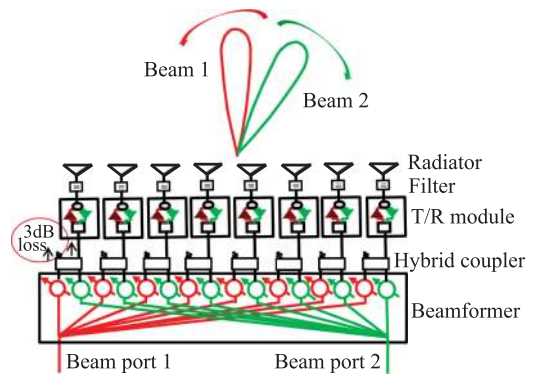


**FIGURE 1. Lossy\* conventional analog single polarized active array beamforming network for two agile beams. (\*) The losses come from the beam combining (or splitting in receive) stage. The beamformer in Fig. 1 itself is not lossy, but the beamforming is (as in Blass matrices [43]). This is due to the couplers placed outside the beamformer. More discussions on definition of orthogonality and losses are given in Section II-C.**

Therefore, the future of both space and cellular communications will need more flexibility, frequency re-use (through spatial multiplexing) and power efficiency at space and ground levels with low complexity [20], [35]. The antenna challenges are to limit gain and power efficiency losses due to array amplitude tapers, beam cross-overs, and to greatly reduce the side lobe interference accumulation at each user, occurring in current systems employing multiple beam forming matrices [8]. Furthermore, the need for efficient and flexible adaptive multiple beam forming with co-channel interference suppression in future satellite communications at space [36], [37] and ground [38] segments is well recognized [39]. Similarly, 5G mobile communications base stations and user equipment require multiple beams and low interference.

A straightforward way of designing a multiple beam former is to have a dedicated beamforming network for each separate beam port and to use power dividers/combiners behind each antenna element. This topology is generally referred to as the “fully-connected architecture” in the literature [18], [40]. A two beam network illustration of such a configuration is given in Fig. 1. Despite being flexible on adjusting the array excitation weights, the fully-connected architecture has a major disadvantage of being lossy, which could be severe especially with more than a few beams. The combining/dividing losses (equal to  $10 \log(N_b)$  for  $N_b$  beams) have to be compensated by an increase of amplifier gain at the element level [3].

A necessary condition to obtain a lossless (ideally) multiple beam forming network is that the beams are orthogonal (in a complex inner product sense) [41]. However, the fact that the beams are orthogonal is not enough to guarantee that the beam forming network is lossless. In other words, a lossy network can generate orthogonal beams as well since vectors do not need to have equal magnitudes to be orthogonal. Then, the transfer block of the scattering matrix (i.e. the block matrix representing beam-port to array-port transfer coefficients) will

not be unitary anymore, but its column vectors will still be orthogonal, corresponding to the distinction between orthogonal and orthonormal vectors terminology<sup>1</sup>. Besides, orthogonality does not necessarily mean that for each beam, signals incident from, or transmitted towards, the other beam peak directions will be zero (as with a Butler matrix [42]). The interference-free system is generally achieved and maintained via flexible (ideally) zero-forced, or very low sidelobe, beams, for which the peak of one beam is at the same angle with (or close to) the null of all the other beams. In general, it is required to have flexibility on the main beam angles while maintaining accurate zeros at the other beam peaks. This requires reconfigurability in the beamforming network. At the current stage, for more flexibility on the angular position of each zero-forced beam, either digital beamforming with increased complexity/cost is employed or highly lossy networks (as in Fig. 1, with combining losses of  $10 \log(N_b)$  dB for  $N_b$  beams) are used in analog beamforming.

It is noticeable that the use of the term “orthogonal” is misleading in many cases in the literature and the authors from different disciplines may actually refer to different scenarios defined by orthogonality. In this paper, the aims are: (i) to highlight the differences between orthogonal beams and zero-forced beams, (ii) to briefly explain the relation between the three concepts extensively used in linear microwave circuits; orthogonality, losses and reciprocity, from an antenna perspective, (iii) to review the literature on orthogonal beamforming networks and flexible zero-forced beamforming architectures, (iv) to show the potential use of orthogonal beamforming and zero-forced beamforming in the signal processing domain for communication system studies, and (v) to provide the reader with insights, future research directions and foreseen challenges.

It is important to be aware of the fact that many studies in the literature wrongly refer to the zero-forced beams as orthogonal beams, which may cause confusion. On the other hand, the zero forced beam phrasing used in this paper has a direct similarity with the zero-forcing terminology that is widely used in the array signal processing community as a precoding strategy [44]. The correspondence is valid in line-of-sight scenarios and when the beam spacing is large enough (more than the angular resolution of the beam,  $\approx \lambda/D$  where  $\lambda$  is the wavelength at the operating frequency and  $D$  is the array length) to guarantee sufficient antenna gain at the main beam positions [45], [46].

<sup>1</sup>In this respect it is worth noting that there are subtle differences in the mathematical terminology referred to inner product spaces and their representing matrices,  $T$ , corresponding to the vectors projection on a complete orthonormal base which span all the space. If the inner product is defined with complex conjugation, the representing matrix of set of orthonormal vectors is a unitary matrix  $TT^H = I$ . On the other hand, if the vectors in the inner product are not complex conjugated, the representing matrix of set of orthonormal vectors is an orthogonal matrix,  $TT^T = I$ . In the following we will address the properties of orthogonal beams and relevant beamforming networks. Orthogonality of the beams and relevant excitations should not be confused with the orthogonality, in matrix sense, of the transfer block of the scattering matrix.

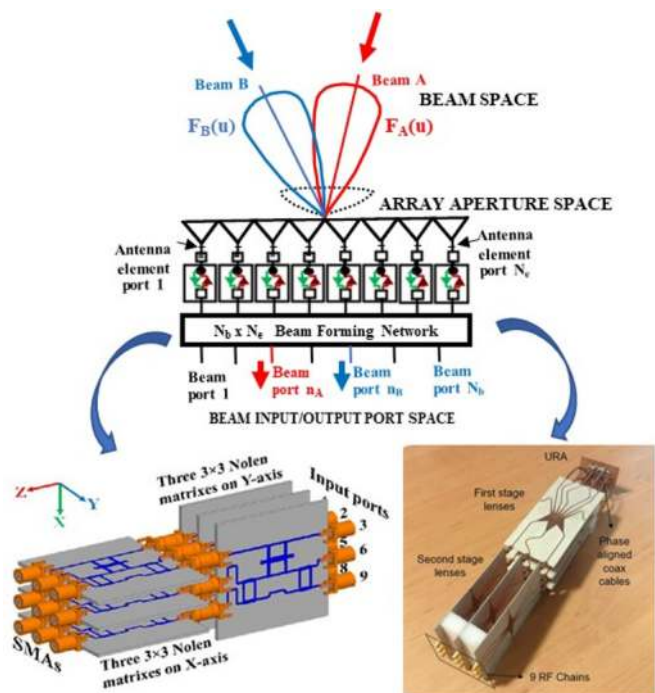


**FIGURE 2.** A generalized multiple beam former and two examples of implementations: using microwave circuit components [47] (on the left), and using Rotman-like lenses [48] (on the right).

The rest of the paper is organized as follows. Section II is dedicated to the comparison of orthogonality and zero-forcing. In Section II-A, the concept of orthogonality in multi-beam antennas is revisited. In Section II-B, the difference between orthogonal beams and zero-forced beams is explained and illustrated. In Section II-C, the intriguing relation between orthogonality, beamforming network losses and reciprocity is discussed from the antenna perspective. In Section III and Section IV, many distinct examples are shown for orthogonal beamforming networks and flexible zero-forced beamforming strategies, respectively. In Section V, the use of orthogonal beamforming and zero-forced beamforming in a communication system is described via several key studies in the literature. In Section VI, future research directions and challenges on the topic are described. Finally, in Section VII conclusions are drawn.

## II. ORTHOGONALITY VS. ZERO-FORCING

### A. DEFINITION OF ORTHOGONALITY

In linear algebra, orthogonality is clearly defined. In Hilbert spaces [49], [50], two vectors  $\mathbf{a}$  and  $\mathbf{b}$  are orthogonal when their inner product  $\langle \mathbf{a}, \mathbf{b} \rangle = 0$ . For a multiple beam array antenna as shown in Fig. 2, this can be applied in the antenna beam port space, its radiating aperture space and its far field radiation beam space, which are Hilbert spaces linearly mapped from one to the other by beam forming and by radiation/scattering operations. The norm  $\|\mathbf{a}\|$  of a vector, is

derivable from  $\|\mathbf{a}\|^2 = \langle \mathbf{a}, \mathbf{a} \rangle$ . Using appropriate inner products,  $\|\mathbf{a}\|^2$  can represent the power applied (or received) at a beam port, reaching the antenna aperture surface or radiated by a particular beam. Linearity/superposition, reciprocity and energy conservation mechanisms can be included in these transformations, for microwave circuit or lens-based beamformers (as illustrated in Fig. 2) and taking into account losses as well as the gain of the amplifiers. Advantages and limitations of Rotman lens-based beamformers are discussed in [48]. Their main advantage over microwave circuit based ones is the bandwidth of the lens, due to its use of time delay rather than phasing. The larger insertion and spill over losses of the lens can be compensated by increased amplification at the element level.

Still, there is no standard (IEEE) definition of antenna beam orthogonality. Most past related work applies to fixed multiple beams, not to adaptive ones and authors vary in their definitions.

According to [41], true orthogonal beamforming is achieved with a lossless (ideally) simultaneous multiple beamformer, with zero (ideally) coupling between the beam ports. According to [51], a multibeam system is truly orthogonal when both criteria below are satisfied:

- (C-i) No internal coupling between antenna ports (generally termed as isolated/decoupled ports in the literature), which means that the pairwise complex dot-products of the excitation vectors for different beams are zero.
- (C-ii) No coupling or interference through radiated field, which means that the average complex inner product of the pairwise radiation patterns is zero.

The above beam coupling terminology and its relation to interference is rather confusing. If the beam weight vectors of two beams using the same radiators, are orthogonal, they can originate losslessly each from one of two separated beam ports, through a cascade of lossless, isolated and completely matched  $2 \times 2$  directional couplers, each equipped of a phase shifter. In this case, the inner product of the beams will automatically be zero.

It can be seen that the conditions, (C-i) and (C-ii), are connected through a Fourier Transform (FT) and thus, can be represented by the same mathematical constraint. Let us consider an aperture of length  $L$  with the one-dimensional aperture distribution of  $g(x)$ . In this case, the radiated field,  $F(u = \sin \theta)$  is computed as

$$F(u) = \int_{-L/2}^{L/2} g(x) e^{jkxu} dx \quad (1)$$

where  $k$  is the wavenumber.

As represented in Fig. 2, to generate two (similar-shaped) beams  $A, B$  with the peaks towards  $\pm u_0 = \sin \alpha$  for an arbitrary angle  $\alpha$ , the required aperture distributions are represented as

$$h_A(x) = g(x) e^{jkxu_0}, \quad h_B(x) = g(x) e^{-jkxu_0} \quad (2)$$

According to (C-ii), the orthogonality is achieved when the following relation holds (assuming  $u \approx \theta$  [41])

$$\int F_A(u) F_B^*(u) du = 0 \quad (3)$$

where  $F_A$  and  $F_B$  are the patterns corresponding to the excitation from the ports of the beams  $A$  and  $B$ , respectively. The sign ‘\*’ denotes the complex conjugate. Note that this condition is valid for beams close to boresight and is linked to angles close to boresight, with the approximation  $\theta \approx \sin \theta$  being valid for small values of  $\theta$ . This also requires the beams to be narrow, so that the angular range considered with the main beam remains relatively close to boresight.

The patterns  $F_A$  and  $F_B$  in (3) are given by

$$\begin{aligned} F_A(u) &= \int_{-L/2}^{L/2} g(x) e^{jkx(u+u_0)} dx, \\ F_B(u) &= \int_{-L/2}^{L/2} g(y) e^{jky(u-u_0)} dy \end{aligned} \quad (4)$$

Then, (3) can be expressed<sup>2</sup> as [41],

$$\int_{-\infty}^{\infty} \int_{-L/2}^{L/2} \int_{-L/2}^{L/2} [g(x) g^*(y) e^{jku(x-y)} e^{jku_0(x+y)}] dx dy du = 0 \quad (5)$$

As the integral with respect to  $u$  gives a Dirac delta function, (5) can be written in a simpler form as

$$\int_{-L/2}^{L/2} g(x) g^*(x) e^{jkx2u_0} dx = 0 \quad (6)$$

It can be seen that (6) is the first condition of orthogonality (C-i) given in [51]. For array antennas, (6) can be interpreted in a discrete form as the complex dot-product of the excitation coefficients for the two beams  $A$  and  $B$ . Thus, (C-i) and (C-ii) represent the same concept, which lies behind the general definition of orthogonality in inner spaces.

By comparing with (1), it is observed that the integral in (6) shows the pattern of the aperture distribution of  $|g(x)|^2$  at the angular location  $2u_0$ . Therefore, to have the integral equal to zero, the inter-beam spacing of  $2u_0$  should be located at the null of the pattern corresponding to the aperture distribution of  $|g(x)|^2$ . For uniform illumination, i.e.  $|g(x)| = 1$ , the orthogonality condition results in the angular inter-beam spacing of  $n\lambda/L$  (for  $n = 1, 2, 3, \dots$ ). This is illustrated in Fig. 3.

There are several other key studies in the literature that focused on the theory of orthogonality in linear and planar multibeam antennas [50]. In [52], it was also concluded that to form simultaneous multiple beams in a lossless manner, the beams must be Hermitian orthogonal, which puts a strict constraint on the excitation coefficients. Later, in [53], [54], it was shown that the truly orthogonal beam positions must satisfy

<sup>2</sup>in the simplifying assumption that the integration of the radiation pattern can be extended outside the visible space,  $|u| \leq 1$ , to the reactive energy domain,  $|u| > 1$ .

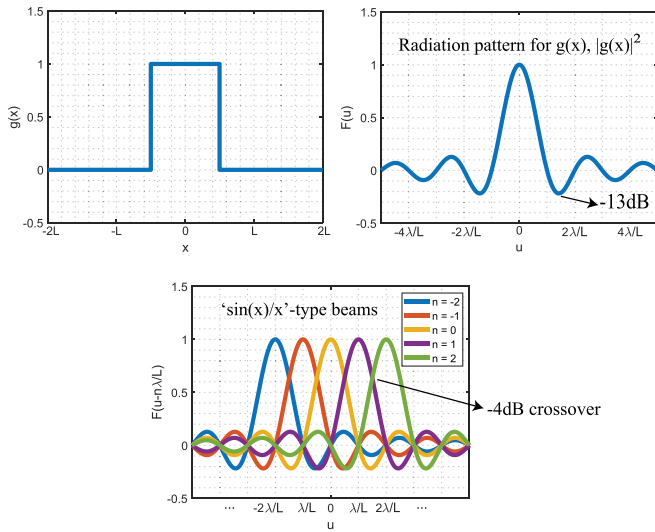


FIGURE 3. Orthogonality properties for uniform illumination.

certain reciprocal lattice conditions and that the phase steering vectors of the lossless beamforming network must correspond to the multi-dimensional Discrete Fourier Transform (DFT).

### B. DOES ORTHOGONAL MEAN ZERO-FORCED?

An important, and commonly misinterpreted, aspect of orthogonality in the recent publications on multibeam antenna systems for future wireless networks is the inter-beam interference. In order to achieve (mutually) interference free transmissions in a one beam per user multibeam system, it is required that, for each beam, signals incident from or transmitted towards the other beams' (peak) directions be zero. Due to the mixed terminology used in the literature, such interference-free beams are renamed as Zero-Forced (ZF) beams in this paper. For the case of uniform illumination with  $|g(x)| = 1$  discussed before, the orthogonal beams  $A$  and  $B$  are spaced in such a way that the spacing is coincident with the zeros of the basic radiation pattern  $F(u)$ . However, this is not always the case since the orthogonality condition (C-i,-ii) only define the beam coupling in terms of excitations' or patterns' overlap. For the complex-valued radiation fields used in (3), the fast variations in phase in the integrand may yield a zero result [55].

As a straightforward but not widely seen example, consider that the beam ports of orthogonal/decoupled/isolated beams  $A$  and  $B$  are connected to a 3 dB hybrid coupler and the two output ports are properly phased to obtain the new beam ports, let us define them as  $C = (A + jB)/\sqrt{2}$  and  $D = (A - jB)/\sqrt{2}$ . In this configuration illustrated in Fig. 4, the aperture distributions (in accordance with (2), for  $|g(x)| = 1$ ) for beam  $C$  and  $D$  are given by

$$\begin{aligned} h_C(x) &= (e^{jkxu_0} + je^{-jkxu_0})/\sqrt{2} \\ h_D(x) &= (e^{jkxu_0} - je^{-jkxu_0})/\sqrt{2} \end{aligned} \quad (7)$$

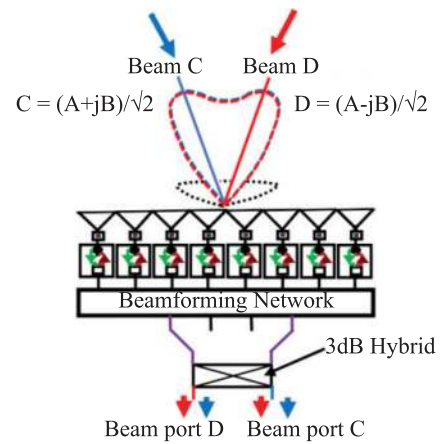


FIGURE 4. Formation of orthogonal (yet spatially overlapped) beams.

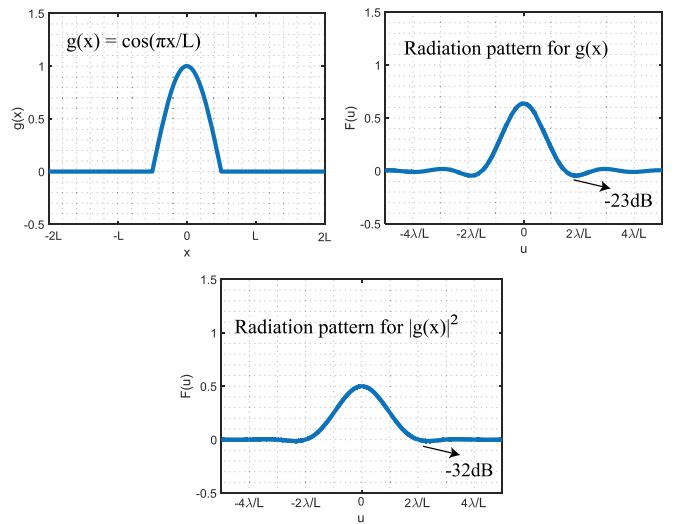


FIGURE 5. Orthogonality properties for cosine-type illumination.

In line with the formulation of (6), the new orthogonality condition for the two aperture distributions is expressed as

$$\int_{-L/2}^{L/2} \cos(kx2u_0)dx = 0 \quad (8)$$

which is again true when the beam spacing of  $A$  and  $B$ ,  $2u_0$ , is equal to an integer multiple of  $\lambda/L$ . Thus, the beams  $C$  and  $D$  are also orthogonal/decoupled/isolated, but this time not ZF. In fact, the two new beam ports produce the exact same gain patterns. A related reference on this is the dual mode antenna using shaped oversized reflectors [56].

Another example could be to assume a non-uniform aperture distribution (i.e.  $g(x) \neq 1$ ). For instance, the pattern nulls for  $g(x) = \cos(\pi x/L)$  correspond to  $u = (n + 0.5)\lambda/L$ , while the orthogonal beam spacing is equal to  $u = (n + 1)\lambda/L$ , for  $n = 1, 2, 3, \dots$ . This phenomenon is shown in Fig. 5. Following the same reasoning, it can be seen that truly orthogonal multiple beam formers that suppress the sidelobes generally

result in low beam crossovers (for the  $g(x) = \cos(\pi x/L)$  distribution, we obtain  $-23$  dB sidelobe level but with  $-9.5$  dB crossover level). Therefore, for the applications that require low sidelobes and high crossovers, lossy networks are generally used, and the losses are compensated by the power amplifiers at the element level [3], [8], [57].

Some disconnect has been observed between definitions and emphasis in the microwave/antennas and the digital communications/signal processing literature. This is apparent in the above discussion on orthogonal and zero-forcing beam forming. Array microwave beamforming networks (as shown in Fig. 1) can simultaneously produce multiple independently agile pencil beams (potentially with Rayleigh angular resolution), as well as reconfigurable shaped or multi-lobed beams. For each beam, weights with adjustable (usually quantified) amplitudes and phases, or time delays, can be computed and refreshed to meet service requirements of several co-channel and other users simultaneously. To meet these needs, microwave beamforming can generate beam excitation functions ranging from uniform (power efficient) amplitudes or tapered ones (for low sidelobes) with planar phase fronts for pencil beams to slightly tapered amplitudes with nearly planar phase fronts for zero forced beams, or synthesized amplitude and phase excitations for shaped or multi-lobed beams.

Unlike time shifters, phase shifters typically provide the same weight phases within each beam sub-band. This creates a problem in applications with multiple paths of unequal lengths, and therefore transit times, both in the receive and transmit modes. Creating, in the directions of the resolvable paths with the strongest signals, pencil beams, preferably zero-forced in all other co-channel path directions, and then time synchronizing, weighing and constructively combining the signals to and from those beam ports is a complex solution. Moreover, in the transmit mode, the loss of combining  $N_b$  beam RF signals into each antenna element power amplifier,  $10 \log(N_b)$ , becomes prohibitive for high numbers of users and multiple paths, and must be compensated by more power amplifier gain.

In principle, digital beam forming allows to implement any beam excitation function achievable with the analog beamformer, without its combining loss. In addition, digital beam forming, with more flexibility, allows to integrate in the precoded signals the time synchronisation and constructive combination of same user signals along their different paths as well as the zero-forcing to reduce co-channel interference. The generic analog solution, as described in Fig. 1, can indeed produce any amplitude/phase excitation required. Constraints are introduced by specific types of microwave beamformers, such as Butler matrices, etc., with the benefit that these specific solutions do not introduce recombination losses. Thus, one ends up with the typical trade-off between flexibility and performance, with higher flexibility leading to higher losses.

However, while analog beamforming solutions require one converter per beam, the digital solutions require one per element. When the number of elements is much larger than the

number of beams, this brings a clear penalty in the power consumption and cost, partly offset by the suppression of the phase shifters (although their consumption is generally quite small, but again magnified by the number of elements, this may be non-negligible). Hybrid beam forming, with a reduced number of RF up/down conversion chains, each connected to subsets of the complete array elements via analog precoders, cannot provide the same coverage performance as the fully-digital or even the analog beamforming but might be a competitive solution for the mid-term.

### C. ORTHOGONALITY, LOSSES, AND RECIPROCITY

The strong constraints on the beam shape, side lobe level, beam pointing, etc. that are imposed by a theoretically lossless orthogonal beamformer design were discussed in Section II-A.

It is important to notice that all beamforming networks using matched and isolated  $n$ -port couplers and phase shifters are automatically producing orthogonal beams, if each beam port is connected to array elements and not to loads [58]. In these networks, there are three spaces: the beam port excitation space, the antenna/array surface illumination space and the beam space. Transformations between these are typically rotations. Thus, orthogonality in the beam port space is preserved at illumination and at beam levels. The square beamforming matrices with such property are commonly referred to as orthogonal beamforming matrices in the literature. On the other hand, there is no standard terminology used for the rectangular counterparts which are called orthogonal beamforming matrices, orthonormal beamforming matrices or beamforming matrices with orthonormal/orthogonal columns/rows in different sources.

The connection between orthogonality and losses is not obvious. One can maintain perfectly orthogonal (and ZF in the case of a Butler matrix) beams, while inserting equal attenuators before each element port. In other words, a beamforming network producing orthogonal beams will still maintain the orthogonality if attenuators are added at the element ports. Similarly, the attenuators can be placed at the beam ports, which do not need to be equal for the beams to remain orthogonal.

For reciprocity, let us consider a system/circuit that includes the receive beam ports,  $r = 1 \dots R$  and transmit beam ports,  $t = 1 \dots T$ . Let us focus on a cellular communication scenario with a base station and phone users. On transmit, the base station sends the signal  $a_t$  from each port  $t$ , resulting in a beam, or outgoing spectrum of plane waves all around. The user  $r$  receives one plane wave, of which he captures/receives some local power and a signal voltage  $b_r$  ( $b_r = \sum_t S_{rt} a_t$ , where  $S_{rt}$  is the base station to users transfer block of the scattering matrix of the system<sup>3</sup> and not that of the base station's beam forming network). On receive, it is the user  $r$  who transmits a signal  $a_r$ . The user does not send back a plane wave, as he had received, but his own beam pattern plane wave spectrum,

<sup>3</sup>known also as base station to user channel matrix.

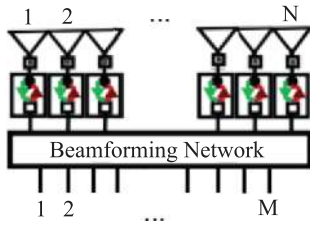


**FIGURE 6.** A generalized multiple beam forming network.

of which the base station receives only one bit of one plane wave and beam port  $t$  captures some power and a voltage  $b_t$  ( $b_t = S_{tr}a_r$ ). Reciprocity says that  $S_{tr} = S_{rt}$ . If now we allow the user to change his direction vector seen from the base station, moving on a sphere around it, and pointing at it,  $S_{rt}$  becomes  $S_{rt}(u)$ , the transmit pattern of that base station beam port. Similarly on receive  $S_{tr}(u)$  will be the receive beam of port  $t$  of the base station. It is because, for each direction  $u$ ,  $S_{tr} = S_{rt}$  so that the transmit and receive patterns of the base station for a beam port  $t$  are the same. Thus, antenna transmit and receive operations are not reciprocal, although reciprocity applies to them. What would be really reciprocal of transmitting out a signal through an (array) beam would be to reverse its propagation flow, recreating in this receive mode the conjugate of the transmit (array) illumination back.

A detailed discussion on reciprocity and losses in terms of the behavior of the beamforming network in the transmit and receive modes was presented in [59]. As the most critical observation of the discussion, it was indicated that there is a possibility to have different levels of internal losses in the network depending on the operation mode, which is yet consistent with the reciprocity theorem, such that the internal losses represent the image of the radiated power variations in the transmit mode. This way, the link budget is balanced and reciprocity is verified. Thus, according to the definition proposed in [59], a lossless network in the transmit mode can be lossy in the receive mode. This is readily understood in the case of a  $M \times N$  beamformer (see Fig. 6), where  $M$  is the number of beam ports and  $N$  the number of radiating element ports with  $N > M$ . This beamformer may be a lossless and matched  $N \times N$  Butler matrix with  $(N - M)$  beam ports terminated with loads. The decoupling between beam ports and between element ports, and the orthogonality of the lossless  $N \times N$  beamformer result in lossless operation in transmit for the  $M$  active beams. In receive, some power from incident plane waves is dissipated in the loaded ports, unless the wave comes from one of the  $N$  beam peak directions.

At this point, it is useful to remember that a spectrum of plane waves (beam) is transmitted and that separate plane waves are received which might interfere at the beam ports or not. The apparent discrepancy between transmit and receive losses in [59] comes from the fact that transmitting from decoupled beam ports through a unitary (i.e. with Hermitian orthonormal columns) scattering matrix (with no loss of power

inside the matrix formed by couplers and phase shifters) generates orthogonal array illuminations and radiation patterns. All the input power is radiated, with or without illumination taper. On receive, because of reciprocity, only incident array illuminations that are conjugate of the transmitted ones can focus in the corresponding beam ports, without any loss in the other beam or terminated ports. This is clearly not the case when the incident illumination comes from a single uniform plane wave between beam peak directions or if the matrix creates an illumination taper. The transmit and receive gains are equal in all directions because the beam port receives the convolution (or discrete inner product) of the incoming plane wave array illumination generated on transmit by that beam port. The same phenomenon is seen with scan loss. On receive, from off-boresight with a large element/subarray, some of the incident intercepted power is reflected, whereas a perfect match on transmit can be achieved with all the power radiated, but the antenna is not lossy on receive. A perfect match is also achieved on receive if the incoming plane wave spectrum is the conjugate of the outgoing one on transmit (i.e. the radiation pattern).

Next in this section, a brief complementary mathematical description on the behavior of a multiple beam forming network is given. To prevent any confusion, it is worth to note the following: a feed network is a junction with  $N$  ports and an  $N \times N$  square scattering matrix  $S$  with elements denoted as  $S_{ij}$ . Some,  $N_b$ , are beam ports, some,  $N_e$ , are element ports (note that normally  $N_b \leq N_e$ ) and some,  $N_l$ , usually loaded, can be unused beam or coupler ports. If the network is lossless, it means that all power coming in comes out, whichever way it comes in, i.e. that all  $N$  vectors  $S_j$  (with components  $S_{ij}$ ,  $i = 1$  to  $N$ , possibly including non-zero  $S_{ii}$ 's, or non-zero  $S_{ij}$ 's between beam ports or element ports) are unit norm complex vectors. The beamforming network transmit and receive transfer matrices  $T$  (with elements  $T_{ij}$ ) and  $T^t$  (with elements  $T_{ji}$ ) relate signals coming out of the  $N_e$  radiating element ports,  $i$ , to signals applied to the  $N_b$  individual beam ports,  $j$ , and vice-versa, with simply  $T_{ij} = S_{ij}$ . Unlike its scattering matrix, the beamforming network transfer matrices involving only beam and element ports are rectangular if  $N_b < N_e$ . Then, while it is possible to have all power applied to one beam port come out at element ports, i.e.  $|T_j| = 1$  for beam ports  $j$ , it is clear that  $|T_i^t| = 1$  will not apply, because part of the power applied to element ports will come out of unused ports. The network with  $N_b + N_e$  ports only with the  $N_l$  unused ports excluded, will be lossy and will not have a unitary scattering matrix.

In the above, if the  $N_l$  unused ports are kept and treated as beam ports, then it becomes possible to have  $|T_j| = 1$  and  $|T_i^t| = 1$  ( $T$ ,  $T^t$  and  $S$  can be unitary matrices). As an example, let us take an  $8 \times 8$  Butler matrix (later given in Fig. 9) of which we decide to use only two beams, i.e. two beam ports (assume port 1 and 5 in Fig. 9) and 8 element ports. We can remove the 5 unused couplers and 2 phase shifters, then we will have 6 unused ports which are still part of the lossless junction. The  $16 \times 16$  scattering matrix is still unitary and users

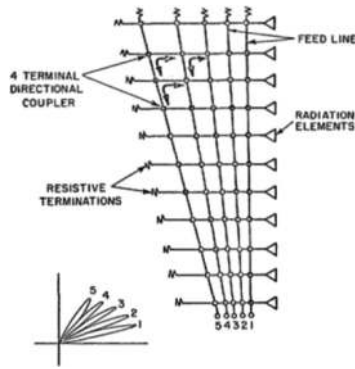


FIGURE 7. The Blass matrix topology [43].

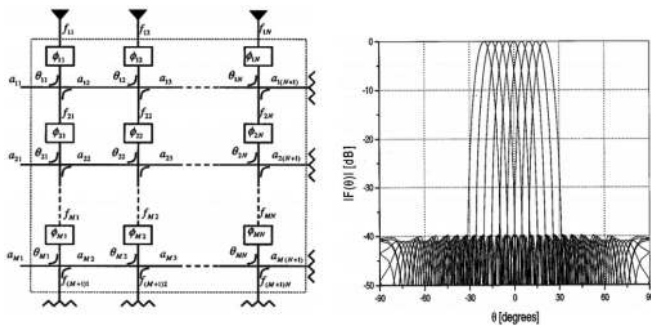


FIGURE 8. The lossy Blass matrix beam-forming network in [60] and corresponding array factor patterns.

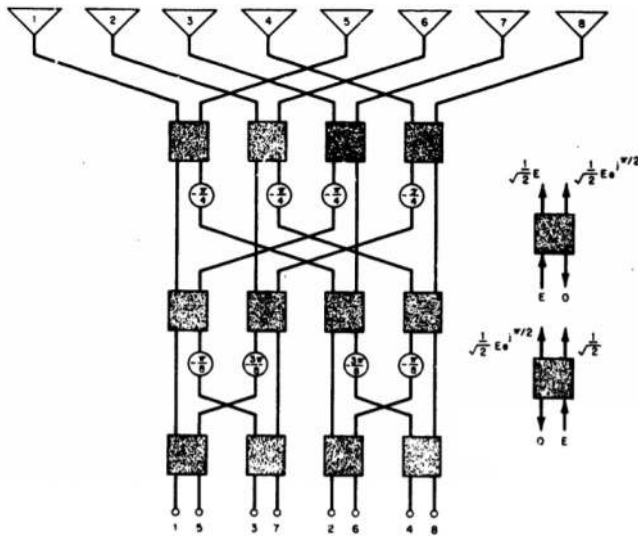


FIGURE 9. An 8-element Butler beamforming network [61].

at the peaks of beams 1 and 5 still have a two-way lossless operation. The power coming from other users will end up in the 2 beam ports and in the 6 unused (loaded) ports with no loss.

However, it is also commonly accepted that the loaded ports are not a part of the transfer matrix, and the matrix is not necessarily square. In other words, the number of input (beam ports) and output (element ports) may differ. In fact, as

explained above, the rectangular transfer matrix is a subset of the complete junction (square) scattering matrix. Therefore, all the information is not there, particularly for receive. More details on such a formulation strategy can be found in [59].

The above considerations on orthogonality, reciprocity, losses and zero-forcing are straightforward, but they are relevant and useful when passive linear analog multiple beamforming networks are used to establish initial designs and trade-offs for multiple beam array designs for transmission of multiple co-channel data streams. In practice, various hardware imperfections and errors from passive and active components and structures, such as amplitude and phase or time delay quantification, non-linearities, thermal effects, variable loading due to coupling for amplifiers or in-phase and quadrature-phase (IQ) imbalance in digital beamforming, will require careful study and calibration schemes to correct their impact on the quality of service.

### III. ORTHOGONAL BEAMFORMING NETWORKS

In this section, a review of the most widely known orthogonal beamforming networks is given from the circuit realization point-of-view.

First, the non-orthogonal Blass matrix was introduced in [43] with no constraints on the output excitations and resulting lossy behavior. A general Blass matrix architecture is given in Fig. 7. Due to the lossy behavior, such a network might be applicable in use cases where power consumption is not so critical [60]. A sample network formulation and resulting multibeam array pattern of a Blass matrix are shown in Fig. 8.

After the introduction of the Blass matrix, there was a growing interest towards the lossless orthogonal matrices [61]. Among them, the well-known conventional Butler matrix was introduced in [42], which typically has the same number of inputs and outputs, equal to an integral power of two. A sample implementation of a standard 8×8 Butler beamforming network is illustrated in Fig. 9.

The standard Butler matrices in planar configurations lead to crossovers in realization, the number of which gets higher with the size of the Butler matrix. The crossover function in a Butler matrix is usually addressed by using two cascaded hybrids [62], [63], which results in an incompact design and larger component count. Motivated by this, more compact single-substrate crossover designs with a broadband operation were also proposed in the literature [64], as seen in Fig. 10. However, single layer 4×4, 8×8 Butler matrix designs without any crossings have been successfully demonstrated as well [65] (see Fig. 11).

It is worth of note that non-standard or oversized Butler matrix realizations can be found in the literature which overcome these design rules. Rectangular Butler matrices with less beam ports than elements are easily obtained by suppressing unused couplers and terminating unused isolated ports [66], [67]. Moreover 3×3, 5×5, 6×6 etc. hybrid couplers and Butler matrices have been introduced in two-dimensional [68]–[71] and three-dimensional [58], [62] configurations. For better



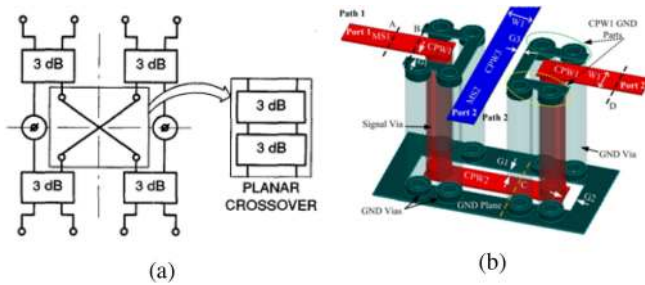


**FIGURE 10.** Sample crossover designs: (a) cascaded hybrids [62], (b) microstrip to coplanar waveguide transition [64].

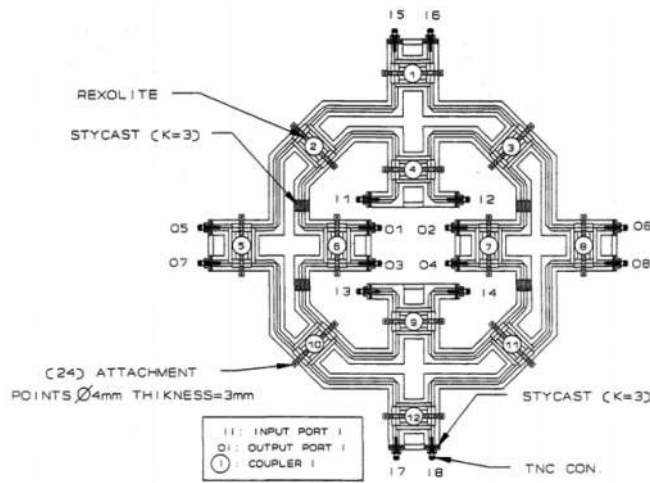


**FIGURE 11.** A single layer 8×8 Butler matrix design at L-band without cross-overs [65].

visualization and understanding, several examples of the non-standard/modified Butler matrices are provided in Fig. 12.

For relatively higher frequencies, the use of Substrate Integrated Waveguide (SIW) technology (advantages and applications of which reviewed extensively in [72]) in the realization of Butler matrices has been proposed. In [73], a low-cost and wideband 4×4 Butler matrix with no crossovers was designed and integrated with slot array elements on the same substrate for radar applications at 77 GHz. In [74], a compact, two-layer, wideband 4×4 Butler matrix in SIW technology was proposed for Ku-band applications centered at 12.5 GHz. The two SIW-based Butler matrix designs in [73], [74] are shown in Fig. 13 for better visualization.

In addition to the conventional Butler matrices with one-dimensional beamforming, Butler matrix networks that are compatible with planar arrays and have the ability to do beamforming in both azimuth and elevation have been proposed in various types. One straightforward way to achieve this is to employ two orthogonal stacks of Butler matrices [75], [76], as illustrated in Fig. 14. An alternative method is the direct two-dimensional beamforming approach using two-dimensional coupler and crossover components [77], [78], which reduces the length of the network significantly. An example from [78] is given in Fig. 15. Such networks generate a square

(or rectangular) lattice of beams, which is not optimal in terms of the crossover between the beams. Recently, in [79], two-dimensional Butler matrices generating a triangular lattice of beams (see Fig. 16 for visualization) was proposed for minimizing the gain roll-off.

A few years later than the introduction of the Blass and Butler matrix, the Nolen matrix was proposed in [80] as an appealing alternative in the sense that it is lossless like the Butler matrix and realized with a serial feeding network without crossovers like the Blass matrix. The Nolen matrix presents a generalized form of an orthogonal multiple beamforming network as it has no limitation on the number of ports. The general architecture of a Nolen matrix is shown in Fig. 17.

Although Nolen-like matrices can provide compact designs, they generally show a relatively narrowband response due to the dispersive behavior with unequal paths from ports to the antenna elements. A sample 4×4 Nolen matrix [81] with the corresponding radiation pattern change in the frequency range of 2.1–2.3 GHz is shown in Fig. 18. Later, in [82], the design rules for cancellation of beam squint with frequency were discussed with a focus on a single-beam four element linear array. The extension of concept to Blass and Nolen matrices was also discussed and it was found that the main limitation originates from the different insertion phase of different directional couplers over frequency.

For higher frequencies, similarly to the Butler matrix implementations, SIW-based Nolen matrix designs have been examined. In [83], a Ku-band 4×4 Nolen matrix (given in Fig. 19) was designed and experimentally validated in SIW technology for the first time. Furthermore, to address the beam squint issue, more “parallel” SIW-based Nolen matrices based on coupler delay compensation were proposed. An example is the broadband 4×4 Nolen matrix presented in [84], the structure of which is shown in Fig. 20 for visualization. In a recent work [85], a compact modified Nolen matrix topology generalized to one-dimensional parallel switching matrices with an arbitrary number of beams was proposed. Its configuration and realization in SIW for a 5×5 parallel matrix is shown in Fig. 21.

Besides the linear array implementations, as seen in the Butler matrices, two-dimensional Nolen matrix networks connected to planar arrays and generating multiple unique radiation beams on azimuth and elevation were also proposed. This function can be achieved by stacking and cascading multiple Nolen matrices. An example of such a design was presented in [47] and shown here in Fig. 22, in which six 3×3 are combined to generate 9 beams.

There are several other works that studied size reduction in Nolen matrices. It was recently shown in [86] that one way to achieve this is to realize each coupler with lumped-elements (i.e. capacitors and inductors). A 3×3 ultra-compact (with 90% size reduction as compared to the conventional designs) Nolen matrix proposed in [86] is provided in Fig. 23 for concept visualization.

In addition to the above-mentioned various types of beamforming matrices with different design goals, modified Butler

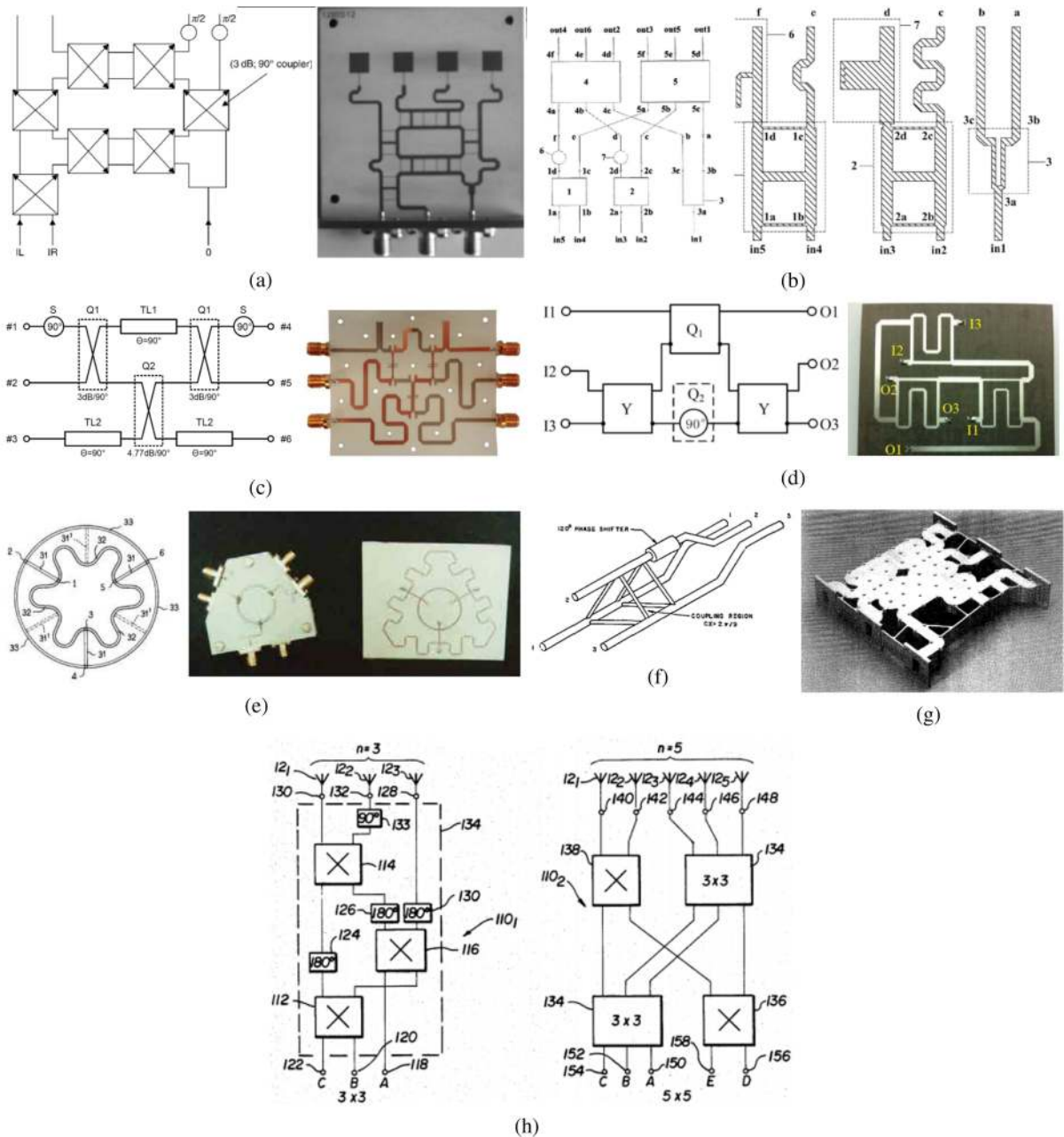


**FIGURE 12.** Non-standard or oversized modified Butler matrix realizations: (a) a  $3 \times 4$  matrix with a broadside beam [66], (b) a  $5 \times 6$  matrix [67], (c) a broadband  $3 \times 3$  matrix [68], (d) a  $3 \times 3$  matrix [69], (e) a printed  $3 \times 3$  matrix [70], (f) a  $3 \times 3$  3D matrix [58], (g) a  $3 \times 3$  matrix in waveguide [62], (h) a  $5 \times 5$  matrix architecture [71].

and Nolen matrix configurations with reduced side lobes were presented in the literature. In the case of the low side lobe Butler matrices, unbalanced power dividers with proper phase compensations are attached to a standard Butler matrix. This way, the number of outputs is increased and desired amplitude law is achieved. A sample modified  $4 \times 8$  Butler matrix design with less than  $-20$  dB side lobes was presented in [87]. The design and pattern results are shown in Fig. 24 for visualization. Another example with an amplitude-tapered Nolen matrix beamforming network was presented in [88] and shown here in Fig. 25. In this case, the matched loads (located at the

bottom four ports in the matrix topology in Fig. 25) dissipate some power in the receive mode with a plane wave incidence. The level of “losses” depends on the angle of incidence (for further information, please see Fig. 5 in [88]).

The multiple beam forming circuits revisited in this section are mainly implemented on printed circuit boards with bulky couplers, except the reduced size matrix realizations. However, for highly-integrated RF systems, there is a growing need for silicon-based implementations. Low-cost is absolutely key for the industry involved, and planar printed antenna with silicon-based RF and processing circuits, like RFCMOS and

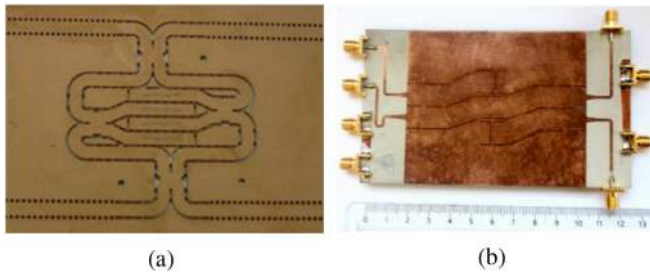


**FIGURE 13.** Butler matrix realizations in SIW technology: (a) a low-cost and wideband  $4 \times 4$  matrix at 77 GHz feeding a slot antenna array [73], (b) a compact and wideband two-layer  $4 \times 4$  matrix at 12.5 GHz [74].

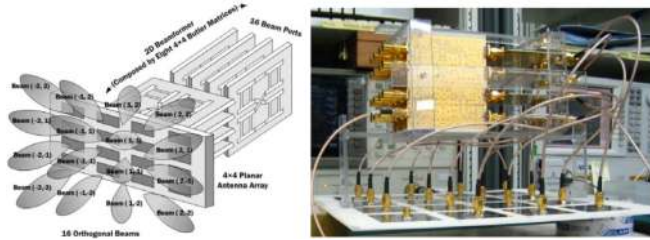


**FIGURE 14.** Two stacks of  $4 \times 4$  Butler matrices at 2.45 GHz generating 16 beam states [75].

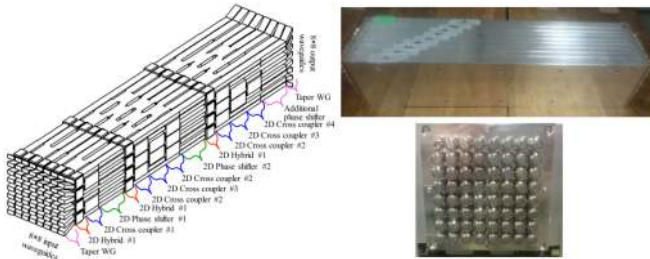


**FIGURE 15.** A  $64 \times 64$  two-dimensional hollow waveguide Butler matrix at 20 GHz using two-plane short slot couplers [78].

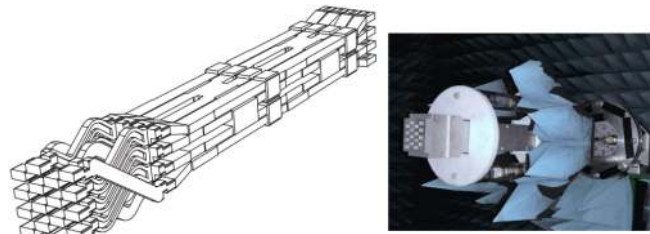


**FIGURE 16.**  $16 \times 16$  connecting network and two-dimensional Butler matrix at 20 GHz generating a triangular lattice of beams [79].

BiCMOS, are a clear option [35]. To this aim, several successful monolithic CMOS Butler matrix designs were reported in the literature [89]–[91]. Fig. 26 gives a visualization of several relevant examples. As mentioned in Section V-B, such matrices can be used as building blocks in a hybrid beamforming system, as proposed in [92] (active sub-arrays with analog beam forming chips, with digitally elaborated sub-array weights at baseband with true time delays). This greatly

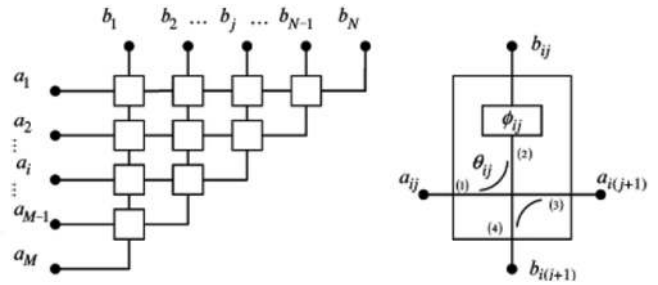


**FIGURE 17.** The Nolen matrix topology [81].

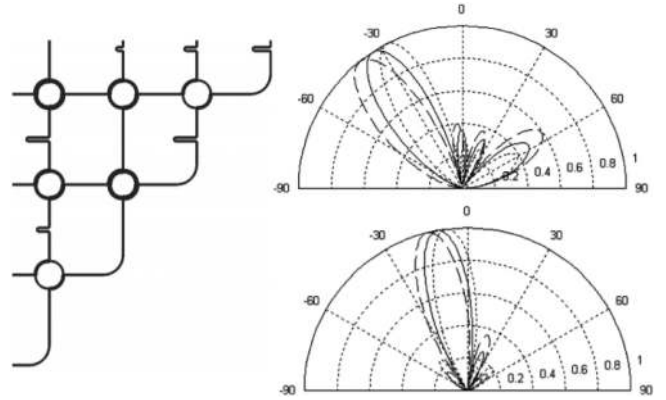


**FIGURE 18.** The  $4 \times 4$  Nolen matrix in [81] and its radiation pattern (for two beam ports) in the range of 2.1–2.3 GHz.

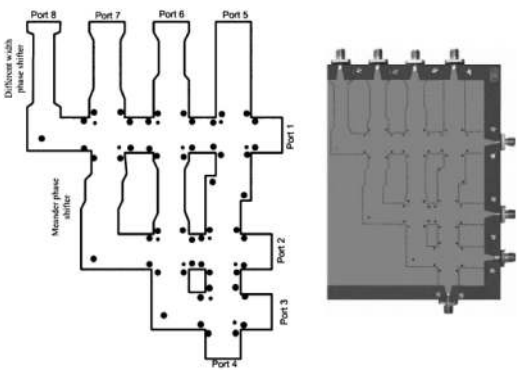


**FIGURE 19.** A  $4 \times 4$  Nolen matrix designed in SIW technology at 12.5 GHz [83].

reduces the number of converters and decreases processing complexity as compared to fully-digital beamforming, while improving the field-of-view, gain and operational bandwidth as compared to the existing analog and hybrid multibeam systems [3].

It is convenient to mention here that multiple approximately-orthogonal beams can also be realized by using lens-fed arrays. A well-known network is the Rotman lens [93], [94]. The original Rotman lens configuration is given in Fig. 27. The interested readers are referred to [95] for a detailed discussion on the development of Rotman lenses. An example lens with an almost half-cosine aperture

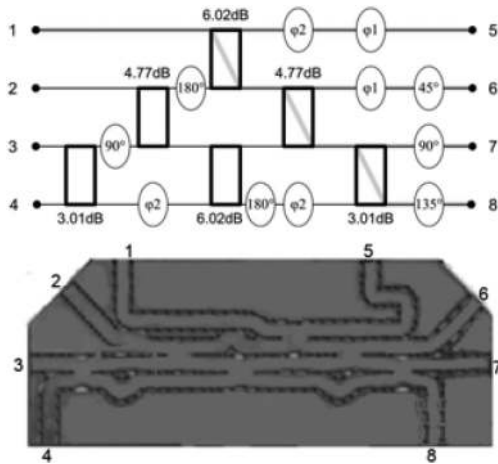


FIGURE 20. A 4 × 4 SIW broadband Nolen matrix designed at 77 GHz [84].

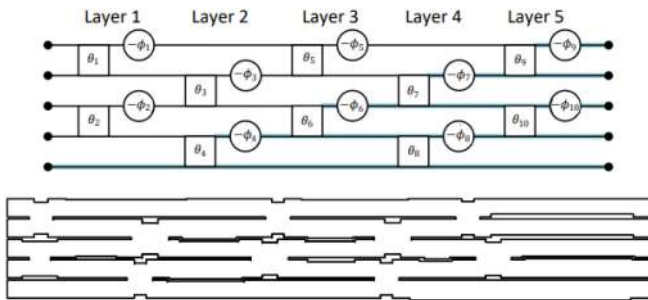


FIGURE 21. A 5 × 5 parallel switching matrix configuration and its realization in SIW technology at 76 GHz [85].

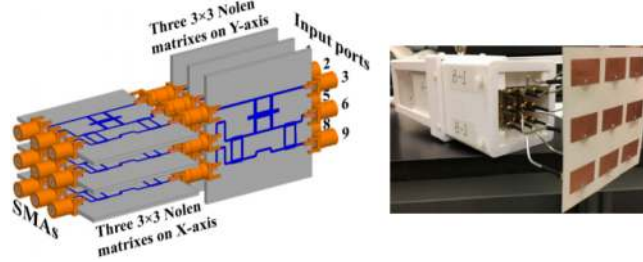


FIGURE 22. The two-dimensional Nolen matrix network connected to a 3 × 3 planar array generating 9 beams at 5.8 GHz [47].

distribution,  $-23$  dB sidelobes and  $-9.5$  dB beam crossovers (recall Fig. 5) was given in [41]. There are several works in this domain which trade off some loss to achieve a higher beam crossover level. Such non-orthogonal beam sets can be achieved with the addition of beam overlap networks as in [96], [97]. More recently, a modified Rotman lens (called as the Fourier Rotman lens) that realizes the Discrete Fourier Transform (DFT) operation (similar to the Butler matrix) was introduced in [98], [99]. The designed Rotman lens structure in [99] and the pattern results are shown here in Fig. 28 for illustration purposes. Such networks are useful as they can provide relatively lower complexity as compared to a Butler

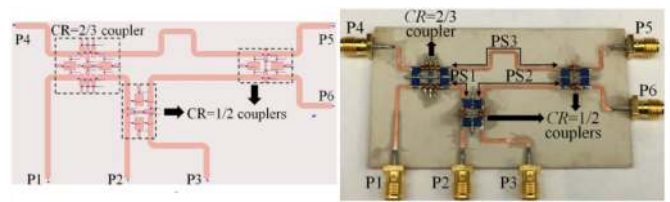


FIGURE 23. An ultra-compact 3 × 3 Nolen matrix design at 1 GHz with lumped-element couplers [86].

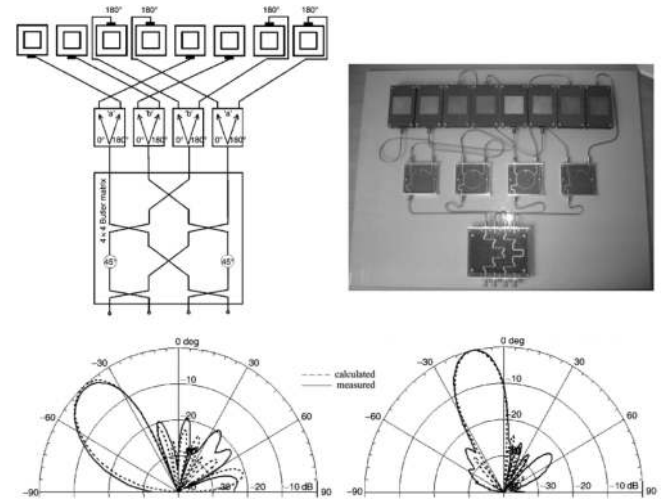


FIGURE 24. A modified 4 × 8 Butler matrix for reduced side lobes [87].

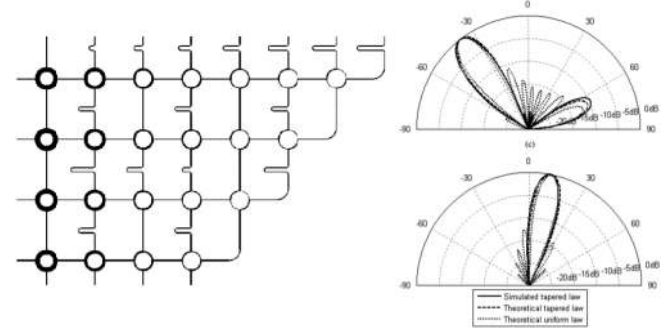
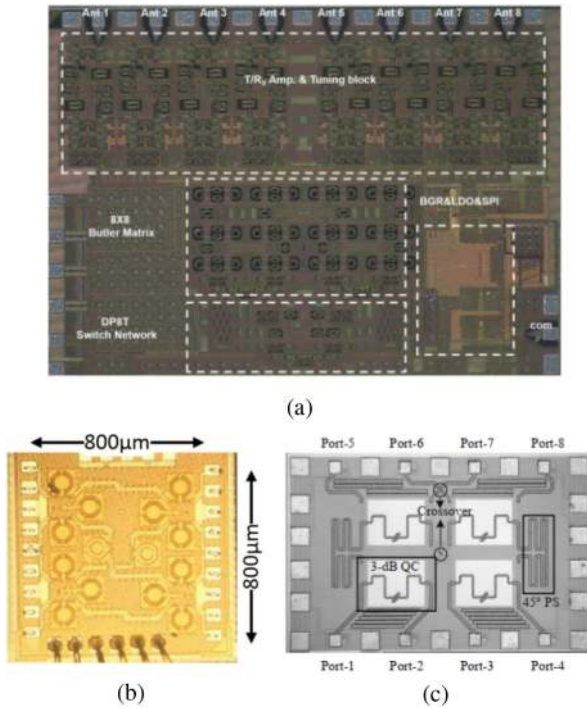


FIGURE 25. A modified 4 × 8 Nolen matrix for reduced side lobes [88].

matrix counterpart when the order of the matrix becomes large.

As a final remark in this section, it is useful to note that the term “quasi-orthogonality” is also encountered in the literature. In these works, the phrase “quasi-” is used to indicate that the orthogonality condition in (6) is partially satisfied as the integral gives a small, yet non-zero, value. In [100], a multibeam mm-wave reflector antenna design was presented for 5G communications. Five quasi-orthogonal beams were synthesized based on the orthogonality criterion such that the inner product of the radiation pattern of two adjacent beams is less than a desired threshold. Fig. 29 shows an illustration of the design and the radiation patterns. In [102], the use of mutually orthogonal radio beams that have a low beam coupling



**FIGURE 26.** CMOS Butler matrix implementations: (a) a 28 GHz  $8 \times 8$  Butler matrix beamformer in 65 nm CMOS process [89], (b) a 9-13 GHz  $4 \times 4$  Butler matrix in 32 nm CMOS Silicon-on-Insulator [90], (c) a 24 GHz  $4 \times 4$  Butler matrix in 0.18- $\mu\text{m}$  CMOS technology [91].

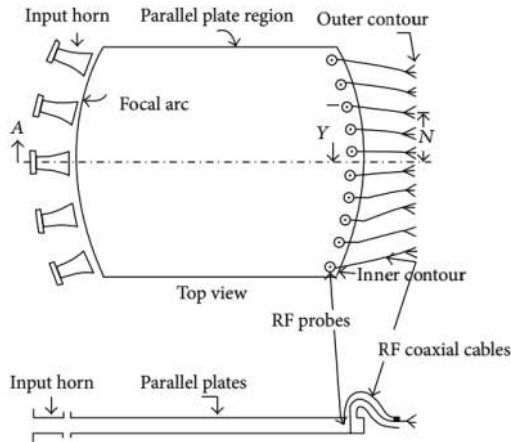


**FIGURE 27.** The original Rotman lens scheme [94].

factor was proposed for radio communication systems. The orthogonal beam space was divided into orthogonal channels, each composed of a few (2 or 3) orthogonal beams. In [101], considering the intrinsic limitations of the orthogonal lossless networks (i.e. maximal number of beams is equal to the number of radiating elements, with an imposed relation between them), the possibility of using dissipative (or lossy) networks with more beams than the elements was investigated. The beamforming network is given in Fig. 30 for visualization. In the final design, a four quasi-orthogonal switching multibeam network (with three orthogonal beams at a desired elevation

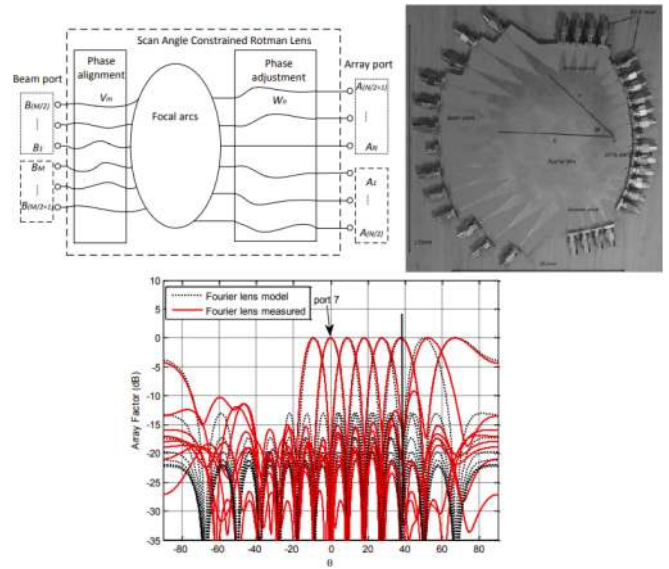


**FIGURE 28.** The Fourier Rotman lens [99].

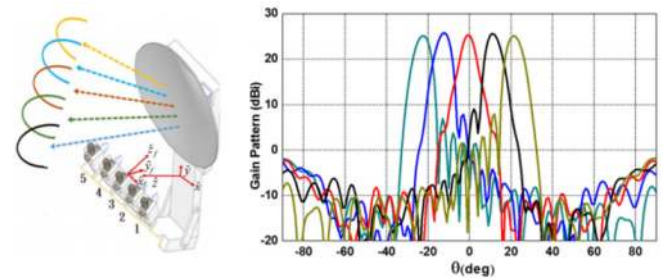


**FIGURE 29.** A multibeam mm-wave reflector antenna with 5 quasi-orthogonal beams [100].

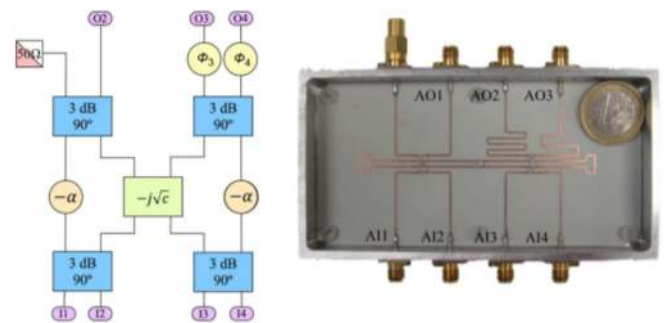


**FIGURE 30.** A  $4 \times 3$  dissipative network for 3 orthogonal beams at desired elevation and 1 beam at broadside [101].

angle and a beam at broadside) was proposed for a triangular subarray of three radiating elements.

#### IV. FLEXIBLE ZERO-FORCED BEAMFORMING NETWORKS

In Section II-B, it was explained that orthogonal beamforming does not necessarily result in zero-forced beams which is crucial to cancel the interference at the beam ports. In Section III, it was seen that standard Butler matrices (or equivalent networks) provide simultaneous orthogonal and

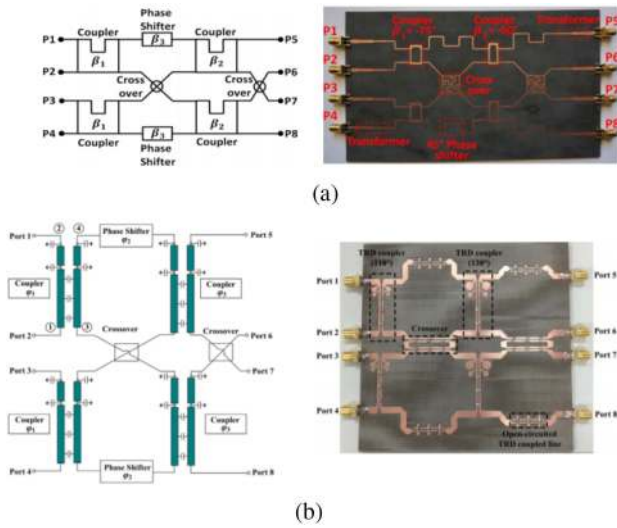


**FIGURE 31.** Flexible phase difference  $4 \times 4$  Butler matrices: (a) [103], (b) [104].

zero-forced beams, yet with strict conditions on the beam spacing.

Several relatively flexible Butler matrices were proposed in the literature [103], [104] which are able to move all Butler beams together without losing the orthogonality. The flexibility is very limited as the beam spacing is kept the same. Besides, the potential use of tunable couplers were mentioned, but not implemented. Two examples of such “relatively-flexible” Butler matrices are given in Fig. 31 for visualization.

In this section, different examples from the literature on the realization of the flexible zero-forced beams are given. Zero-forcing precoding under the domain of digital signal processing is covered in Section V.

In [105], a wideband multibeam MIMO receiver with 4 reconfigurable zero-forced beams was designed (in 22-nm fully-depleted silicon-on-insulator technology) with a flexibly programmable analog beamforming by exploiting a vector modulator. The aim was arbitrary analog interference rejection by spatial notch filtering. The proposed beamforming architecture is given in Fig. 32 for better visualization.

In [106], a generic multibeam architecture (given in Fig. 33) was presented for a satellite ground terminal which is capable of using multiple zero-forced beams to simultaneously communicate with multiple different orbital satellites operating at the same frequency band. Broadly, it was mentioned that the beamforming network can provide fixed, reconfigurable or dynamic beams for tracking and be built in an analogue or digital fashion.

In [107], the zero-forced beam generation concept was verified experimentally by using two well-separated pencil beams in the azimuthal plane at the receiver side. The experimental setup is as shown in Fig. 34. Following the estimation of the angular locations of the transmitters, the dedicated beamforming networks (labeled as OBFM in Fig. 34) were adjusted to receive interference-free information from the

two transmitters exploiting the same time-frequency resource block. Later, the same authors extended their study with an application of zero-forced vertical beams in an indoor communication scenario [108].

In [28], a partially overlapped 64-67 GHz four-element hybrid beamforming receiver fabricated in a 130-nm SiGE BiCMOS process was presented. The null steering performance was demonstrated for the reception of two concurrent streams with two overlapped clusters of elements. The realization of the proposed beamformer architecture and the formation of two simultaneous zero-forced beams are shown in Fig. 35 for visualization.

In [109], a 10 GHz 65-nm CMOS four-element digital beamforming receiver front-end was reported with spatial cancellation of co-channel interferers (of more than 20 dB) at RF. The beamformer topology and its implementation are shown in Fig. 36. The concept was also extended to the cancellation of multiple spatial interference signals which may occur in more realistic scenarios. In [110], a 4-element 0.1-to-3.1 GHz digital beamforming receiver prototype was implemented in 65-nm CMOS technology and the formation of multiple arbitrary notches was demonstrated. The proposed array configuration is given in Fig. 37. A similar example can be found in [111], where a scalable 0.1-to-1.7 GHz spatio-spectral-filtering 4-element digital receiver array implemented in 65-nm CMOS technology was presented.

In [29], a 28-/37-GHz hybrid beam forming receiver (in 65-nm CMOS technology) was designed with four antenna inputs and two baseband output streams. A new technique called time-multiplexed least-mean-square (LMS) was introduced in an RF beamformer for the first time to perform symbol-by-symbol LMS adaptation of the antenna pattern. The adaptation technique was then used to steer both the main lobe and a null when two beams are simultaneously directed to the receiver from two transmitters. The corresponding beam former design and beam patterns are shown in Fig. 38. In [30], the same authors presented a 25–30 GHz fully-connected hybrid beamforming receiver (in 65-nm CMOS technology) with eight antenna inputs and two baseband output streams. To demonstrate the interference cancellation capability, a signal was applied to one element, and a phase shifted version was applied to another element. By combining the two channels, a peak-to-null ratio of 20 dB was achieved.

It is worth to mention that several existing and most related multibeam examples with the demonstration of zero-forced beams have been included here. The list can be broadened with other antenna systems using chipscale multibeam front-ends [112], [113] or hybrid architectures employing analog beamforming integrated circuits [114]–[116], as they can be used for the purpose of flexible zero-forcing with proper array element excitations.

## V. ORTHOGONAL BEAMFORMING AND ZERO-FORCING IN COMMUNICATION SYSTEM STUDIES

In this section, as a complementary and closely related subject, the focus will be more on the signal processing aspects in

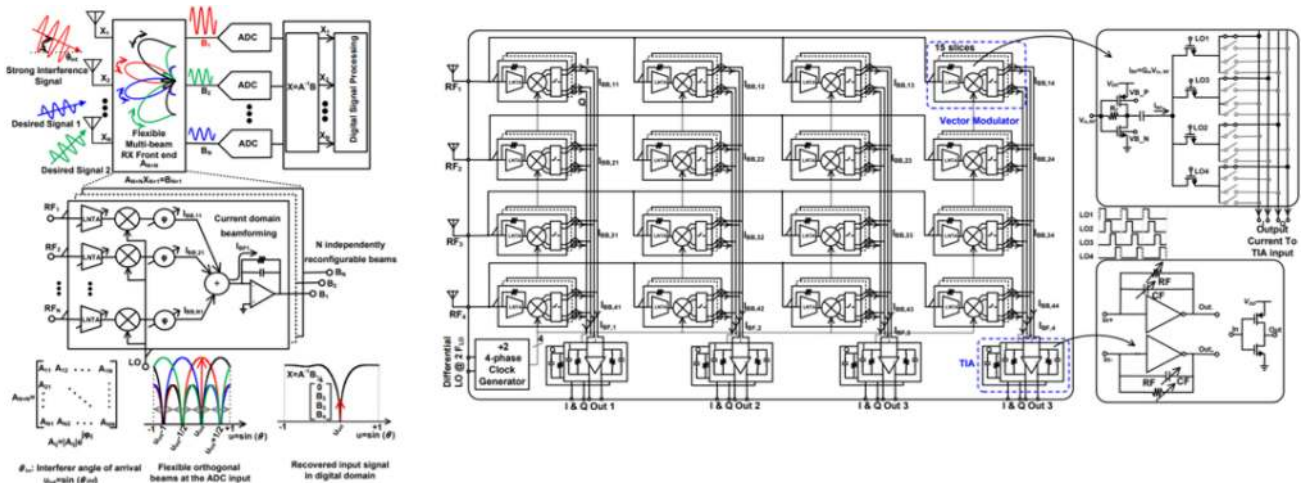


FIGURE 32. A 4 × 4 MIMO receiver with 4 reconfigurable zero-forced beams [105].

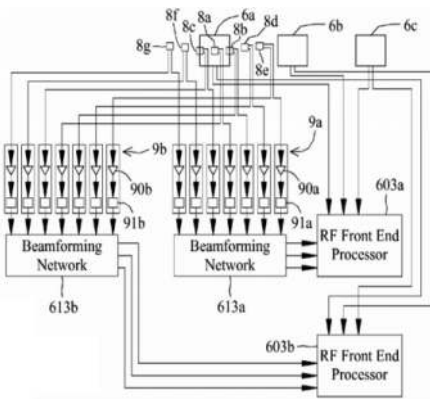


FIGURE 33. Multiple zero-forced beam forming network for a satellite ground terminal [106].

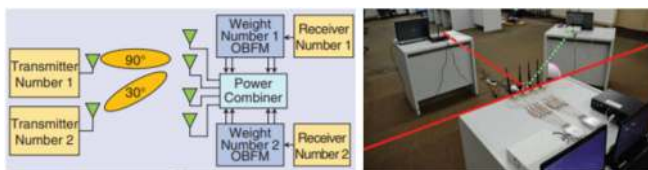


FIGURE 34. Zero-forced beam forming setup for a communication system serving two simultaneous co-frequency users [107].

a communication system employing orthogonal and/or zero-forced beams.

### A. THE USE OF ORTHOGONAL BEAMS

It is known that for conventional precoders (matched filtering, zero-forcing, minimum mean square error), once the user scheduling is performed, the transmitter computes the excitation weights to determine each user's achievable Signal-to-Interference-plus-Noise-Ratio (SINR). In other words, to precisely know the SINR of a user (especially in the case of totally random selection of users), the beamformers need to be

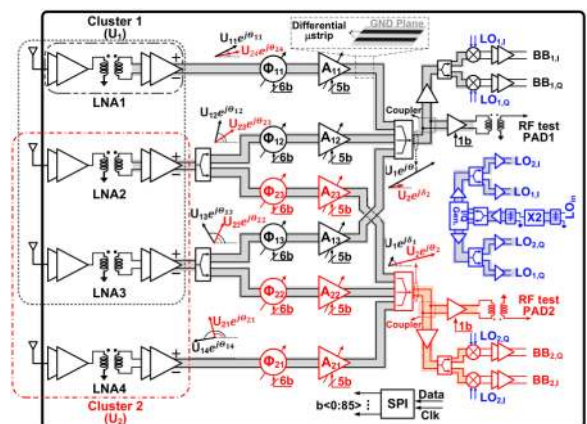
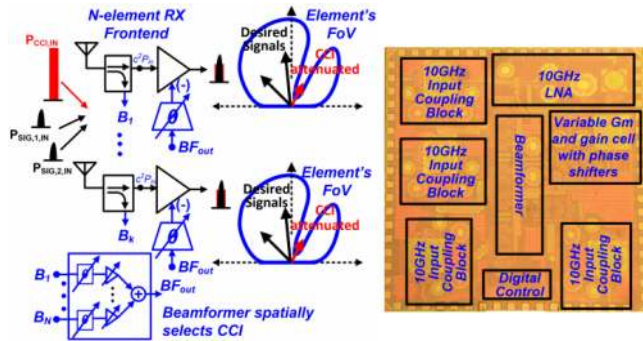


FIGURE 35. The realization of a partially overlapped 64-67 GHz four-element hybrid beamforming CMOS receiver and a sample formation of two zero-forced beams [28].

computed first, which is generally a time consuming and computationally expensive operation. Therefore, with orthogonal beamforming in the signal processing area, it is proposed that the transmitter will use an orthogonal set of excitations for which the inter-user interference and the precise knowledge of SINR can be easily obtained. This way, the aim is to find the optimal user set easily, without computing the complex beamformers.

Following this motivation, in [117], an Opportunistic Space Division Multiple Access (SDMA) algorithm (OSDMA) was



**FIGURE 36.** A 10 GHz four-element digital beamforming CMOS receiver front-end with out-of-beam co-channel interference cancellation at RF [109].

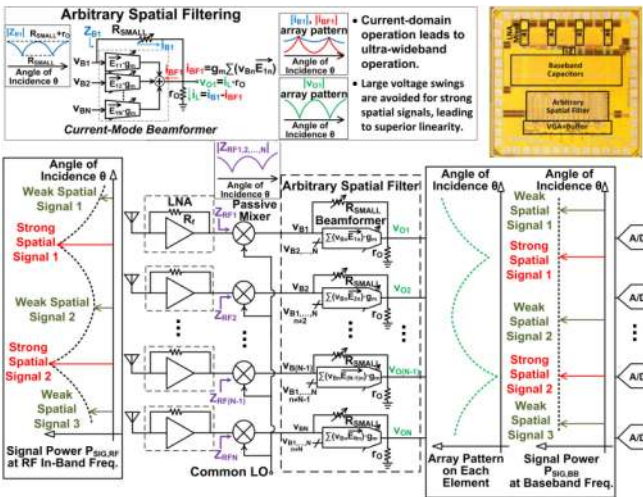


**FIGURE 37.** A 4-element 0.1-to-3.1 GHz digital beamforming CMOS receiver forming multiple arbitrary spatial notches [110].

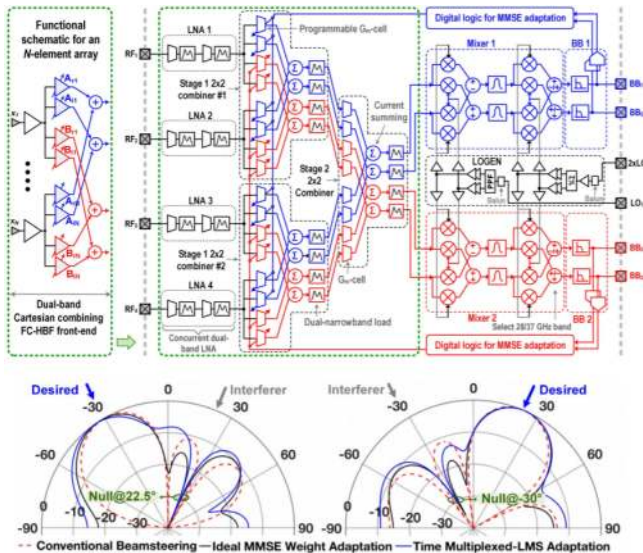


**FIGURE 38.** A 28-/37-GHz hybrid beam forming CMOS receiver with four antenna inputs and two baseband output streams and the corresponding beam patterns assuming a uniform linear array under different beam forming strategies [29].

proposed for MIMO broadcast channels in which the base station sends a number of random orthonormal beams using as many random beamformers as the transmit antennas. Each user feeds back its best beam and its corresponding SINR to the base station. Based on the received SINR's, the base station schedules transmissions to a part of the users. Such a technique was proven to be efficient for a large number of active users. In [118], [119], the idea of random orthogonal beamforming was extended with an adaptive scheme to dynamically control the number of active beams according to the operation environment, which is seen to be useful in sparse networks with low number of users or in the case of uneven spatial distribution of the users.

In [120], the use of orthogonal beamforming vector constraint for transmission (referred to as orthogonal linear beamforming, OLB) was exploited in MIMO broadcast channels using SDMA. Tailored to that, a low-complexity (as compared to the exhaustive search) user selection technique was proposed to achieve the highest sum-rate, based on the exact knowledge of SINR at the transmitter with the orthogonal transmission. Two different algorithms (based on the selection strategy of the basis vector of the orthonormal precoding set obtained via Gram-Schmidt orthogonalization) were proposed to jointly decide on a smart set of the orthogonal vectors to be assigned to the associated users. Through parametric studies, the advantages of OLB in terms of the user scheduling complexity and throughput as compared to the zero-forcing and matched filtering precoding were shown for low-SNR and low number of user scenarios.

Complementary to the work in [120], the optimal choice of the unitary orthogonal vectors regarding the number of feedback bits, the amount of latency, and the sum capacity was investigated later in [121]. The use of partially orthogonal beamforming weights was proposed in [122].

In [123], orthogonal beamforming in space division multiplexing broadcast channels was studied under the name per user unitary and rate control (PU2RC), which was proposed as a 3GPP-LTE standard. The main feature of PU2RC is the orthogonal precoding constraint where each user selects a beamformer weight from a codebook of multiple orthonormal bases, which, from the antenna-system perspective, presents major similarities with the fixed and orthogonal grid-of-beams approach. This is also referred to as limited-feedback OS-DMA (LF-OSDMA) in the relevant literature. Through simulation results, the superior throughput performance and robustness of PU2RC as compared to zero-forcing beamforming was demonstrated for sufficiently large number of users.

Following the work in [123], an improved (in terms of fairness) user scheduling approach for orthogonal beamforming was presented in [124]. The method is based on a round-robin scheduling which uses the CSI to arrange the transmit power among the users so that a given SINR constraint is fulfilled. Through the system simulations, the approach was found to be effective for time-varying channels and in real-time multimedia traffic.



## B. THE USE OF ZERO-FORCED BEAMS

Due to their simplicity from the system management perspective, switched-beam schemes based on fixed orthogonal and zero-forced beams have been widely used in the conventional satellite communication systems and cellular systems. Some examples include ISM-band wireless communications [125] (fixed or hybrid fixed/adaptive beamforming in elevation/azimuth), wideband code division multiple access networks [126] and mm-wave communications [127], [128].

Considering the performance limitations of purely fixed orthogonal and zero-forced beams, several architectures with beam reconfigurability were proposed in the literature. Based on a combination of fixed orthogonal beams and a reconfigurable beamforming network, relatively low-complexity hybrid architectures were introduced, adapted to a direct radiating array [129], [130], to a focused array with multipoint amplifiers [129] and to overlapped subarrays [131]. In [132], an efficient, modular and scalable design solution for reconfigurable beamforming networks was given.

Recently, hybrid beamforming approaches have also been studied that combine the fixed orthogonal zero-forced multiple beamforming with digital precoding for performance improvement [133]. Some examples from the literature employ a large Butler network [134] or a Rotman lens [48] connected to a baseband processor.

In a recent work on a hybrid mm-wave system [135], a single-user scenario was considered with one data stream per each RF chain. The problem of simultaneous clustering of antenna elements both at the transmitter and receiver with optimal precoding associated to the clusters was addressed. The aim was to maximize the signal to inter-subarray (i.e. between the selected transmit and receive subarrays) interference ratio. It was mentioned the study is limited to point-to-point communication and isolated sensor network applications, yet with potential to be extended to multi-user environments including inter-user interference aspects.

In [136] a hybrid beamforming system based on interleaved subarrays was proposed for multibeam multiplexing in arbitrary beam directions. The aim was to achieve much narrower beam widths with the interleaved structure, while avoiding high side lobes and grating lobes through varying/fixed antenna spacing with an associated analog weighting of the subarray elements and a simple digital inter-subarray coding scheme. Through joint optimization of analog and digital coefficients in sample linear and planar arrays, the formation of two and three simultaneous angularly well-separated beams with low interference levels (below  $-20$  dB) were reported, which can potentially be improved by implementing zero forcing based optimization techniques.

Yet, the full-power of zero-forced beams appears when created via fully digital beamforming. For example, in [137], multiple zero-forced beams (up to 5, with full frequency reuse at the same time) were formed digitally at the transmitter side for indoor multiuser wireless communications with a deterministic channel in line-of-sight and in the presence of active

scattering devices. In [138], the “one-beam-per-user” concept was proposed in satellite communications with dispersed and flexible coverage. In this scenario, a large direct radiating array complemented with an adaptive beamforming mechanism provides a maximal gain available by the aperture towards the user of interest, which can improve the link budget by up to 3-4 dB at the beam crossings as compared to the traditional fixed multibeam coverage. At the same time, the co-user (or jamming station) interferences can be rejected effectively with the adaptive zero-forced beamforming. To achieve this in a relatively efficient way, three iterative and fast-converging algorithms (namely conjugate-gradient beamformer, auxiliary-vector beamformer and random beamspace processing) were proposed, the performances of which depend on the presence and the number of interferers. In [139], zero-forced beams were used to optimize the quality-of-service in line-of-sight based multiuser SDMA systems. The impact of decreasing the number of zeros (i.e. complexity reduced zero-forcing [140]) on the SINR and the processing burden was also investigated.

There are also studies which combine the advantages of orthogonal beamforming and zero-forcing precoding in an alternating fashion depending on the changes in the environment. Such a strategy was shown to outperform each individual scheme in all ranges of SNR and number of users [141].

Flexible zero-forced beams are, in general, hard to synthesize and maintain. The system non-idealities, quantization errors and fabrication tolerances may have a strong negative impact on the level of nulls, which may significantly deteriorate the interference suppression performance of the multibeam array. In this case, the throughput performance of the system approaches to the one of the matched filtering, or simple adaptive beam steering [45]. Furthermore, in [142], it was pointed out that the performance (in terms of the bit error rate) of the switched-beam system approaches that of the adaptive beam steering (with more computational complexity) when the spatial beam spacing becomes very small. That is why the grid-of-beams technique with large crossover level is proposed (mostly with digital beamforming due to high losses in the case of analog beamforming), which selects the excitation vector from a pre-defined set [143]–[146]. In the grid-of-beams approach, the beams are not required to be orthogonal or zero-forced and, in principle, an arbitrary number of beams can be generated. In [57], the grid-of-beams method was investigated as a pragmatic approach for massive MIMO in broadband communication satellites. The detailed system analyses presented include critical radio resource management aspects such as the optimal beam spacing, minimum user spacing, per user power normalization, array element spacing, number of array elements, number of simultaneously active users and resource slicing in time and frequency sub-bands. The appealing performance-complexity trade-off with the proposed approach was shown in comparison to the conventional precoding algorithms.

It is worth noting that the study in [57] and most of the current work on the matched filtering precoding or grid-of-beams

use periodic array topologies with high side lobes on average. However, it can be seen that literature is very rich regarding the aperiodic array synthesis techniques [147]–[155] and the multidisciplinary system advantages (on the link quality, computational burden, thermal management etc.) brought by the array layout irregularity [45], [156]–[162]. Motivated by this, recently, the idea of employing optimized coverage-specific aperiodic multibeam array antenna layouts with low side lobes ( $< -30$  dB) and optimal power efficiencies was proposed in [163]. The set of beams generated by such multibeam array layouts can be considered as “quasi zero-forced” due to the very low level of interference between its beam ports. Thus, the computational complexity in precoding can be greatly reduced (with a small impact on the throughput) by using, instead of the zero-forced beams, grid-of-beams or matched filtering combined with the quasi zero-forced beam generating layouts.

## VI. FUTURE RESEARCH DIRECTIONS, BENEFITS AND CHALLENGES

To improve the system capacity and network quality in the future satellite and cellular communication systems, it is required that: (i) the antenna gain is maximized and the total interference is minimized simultaneously towards several beam positions using the same frequency, and (ii) power amplifier efficiency is kept close to optimum to limit consumption. Therefore, the ultimate aim with a flexible multiple beamforming architecture is to generate beams minimizing cumulated co-channel interference of users with arbitrary (but well separated) angular positions over some bandwidth, while approaching to a (theoretically) lossless realization with maximum efficiency. Such an architecture would remove the combining losses of current analogue multibeam active array solutions, while optimizing the array gain, SINR’s and power efficiency.

The potential applications include:

- Future GEO, MEO and LEO satellite payloads for communication to and from mobile or fixed users with high frequency re-use and power efficiency requirements.
- Users of the above communication satellites, in particular for connection to 5G and 6G systems, for which higher gain and therefore agile narrower beam(s) will be needed (e.g. individual satellite tracking and smooth-handover functionality in large LEO (OneWeb, Starlink) or MEO (O3b) constellations).
- Gateways, using one or a few multiple beam array(s) instead of one pointable reflector per satellite.
- Base stations and mobile users of the future 5G and 6G infrastructures.
- Radar systems, in particular to suppress multipath and interferer signals.

Although there are several works that focused on modified Butler matrices with relatively flexible phase differences, to the authors knowledge, these techniques allow all the Butler beams to be moved together; otherwise, the peak gain of one beam no longer corresponds to the nulls of all the other beams

and large interference may occur. Therefore, there is some interest in synthesizing flexible zero-forced beams, realized with a low-loss and non-dispersive matrix, and with reconfigurability on the multiple beamforming network. The major challenges foreseen are in the synthesis of such a beamforming matrix (including practical design factors, mutual coupling), realization in low cost integrated circuit technology and calibration of the network.

## VII. CONCLUSION

In summary, multiple beam generation networks are reviewed from the antenna, electronics and communication system perspectives, with a focus on the distinct properties of orthogonal and zero-forced beamforming. As the terminology is generally confused in the literature, the precise definitions of orthogonal and zero-forced beamforming in multibeam antennas are given. The intriguing relation between orthogonality, losses and reciprocity is explained.

Various examples of orthogonal and flexible zero-forced beamforming networks are shown. Some useful insights on their operation principles, design/implementation, applications and advantages/disadvantages are provided. The review is also tailored to the system level studies including the signal processing aspects.

Furthermore, the applicability of the current technologies in the next-generation satellite and cellular communication applications is discussed. It is pointed out that the demanding high-gain, low-interference requirements of the future wireless systems call for the development of low-loss, non-dispersive and reconfigurable multiple zero-forced beamforming matrices that can be realized in low-cost integrated circuit technology.

## ACKNOWLEDGMENT

The authors would like to thank the anonymous reviewers for their insightful and constructive comments.

## REFERENCES

- [1] W. Imbriale and G. Wong, “An S-band phased array for multiple access communications,” in *Proc. Nat. Telecommun. Conf.*, vol. 2, 1977, pp. 19.3.1–19.3.7.
- [2] R. J. Fang, “Broadband IP transmission over SPACEWAY satellite with on-board processing and switching,” in *Proc. IEEE Glob. Telecommun. Conf. (GLOBECOM)*, Houston, TX, USA, Dec. 2011, pp. 1–5.
- [3] Y. Aslan, J. Puskely, A. Roederer, and A. Yarovoy, “Active multipoint subarrays for 5G communications,” in *Proc. IEEE APS Topical Conf. Antennas Propag. Wireless Commun.*, Granada, Spain, Sep. 2019, pp. 298–303.
- [4] D. Gesbert, M. Kountouris, R. W. Heath Jr., C. Chae, and T. Chae, “Shifting the MIMO paradigm,” *IEEE Signal Process. Mag.*, vol. 24, no. 5, pp. 36–46, Sep. 2007.
- [5] T. L. Marzetta, “Massive MIMO: An introduction,” *Bell Labs Tech. J.*, vol. 20, pp. 11–22, 2015.
- [6] E. Ali, M. Ismail, R. Nordin, and N. F. Abdulah, “Beamforming techniques for massive MIMO systems in 5G: Overview, classification, and trends for future research,” *Front. Informat. Technol. Electron. Eng.*, vol. 18, no. 6, pp. 753–772, Jun. 2017.
- [7] M. Wang, F. Gao, S. Jin, and H. Lin, “An overview of enhanced massive MIMO with array signal processing techniques,” *IEEE J. Sel. Top. Signal Process.*, vol. 13, no. 5, pp. 886–901, Sep. 2019.

- [8] W. Hong *et al.*, "Multibeam antenna technologies for 5G wireless communications," *IEEE Trans. Antennas Propag.*, vol. 65, no. 12, pp. 6231–6249, Jun. 2017.
- [9] G. W. Kant, P. D. Patel, S. J. Wijnholds, M. Ruiter, and E. van der Wal, "EMBRACE: A multi-beam 20,000-element radio astronomical phased array antenna demonstrator," *IEEE Trans. Antennas Propag.*, vol. 59, no. 6, pp. 1990–2003, Jun. 2011.
- [10] H. Steyskal and J. F. Rose, "Digital beamforming for radar systems," *Microw. J.*, vol. 32, no. 1, pp. 121–136, 1989.
- [11] D.-W. Kang, K.-J. Koh, and G. M. Rebeiz, "A Ku-band two-antenna four-simultaneous beams SiGe BiCMOS phased array receiver," *IEEE Trans. Microw. Theory Techn.*, vol. 58, no. 4, pp. 771–780, Apr. 2010.
- [12] K. J. Maalouf and E. Lier, "Theoretical and experimental study of interference in multibeam active phased array transmit antenna for satellite communications," *IEEE Trans. Antennas Propag.*, vol. 52, no. 2, pp. 587–592, Feb. 2004.
- [13] S. S. Ahmed, A. Genghammer, A. Schiessl, and L.-P. Schmidt, "Fully electronic E-band personnel imager of 2 m<sup>2</sup> aperture based on a multi-static architecture," *IEEE Trans. Microw. Theory Techn.*, vol. 61, no. 1, p. 651–657, Jan. 2013.
- [14] W. Menzel and A. Moebius, "Antenna concepts for millimeter-wave automotive radar sensors," *Proc. IEEE*, vol. 100, no. 7, pp. 2372–2379, Jul. 2012.
- [15] L. Zhang, A. Naterajan, and H. Krishnaswamy, "Scalable spatial notch suppression in spatio-spectral-filtering MIMO receiver arrays for digital beamforming," *IEEE J. Solid-State Circuits*, vol. 51, no. 12, pp. 3152–3166, Dec. 2016.
- [16] W. Liang *et al.*, "Field trial investigation of wired and wireless calibration schemes for real-time massive MIMO prototype," in *Proc. IEEE 86th Veh. Technol. Conf.*, Toronto, ON, Canada, Sep. 2017, pp. 1–6.
- [17] Y. J. Guo, M. Ansari, and N. J. G. Fonseca, "Circuit type multiple beamforming networks for antenna arrays in 5G and 6G terrestrial and non-terrestrial networks," *IEEE J. Microwaves*, vol. 1, no. 3, pp. 704–722, Jul. 2021.
- [18] I. Ahmed *et al.*, "A survey on hybrid beamforming techniques in 5G: Architecture and system model perspectives," *IEEE Commun. Surv. Tut.*, vol. 20, no. 4, pp. 3060–3097, Jun. 2018.
- [19] J. Zhang, X. Yu, and K. B. Letaief, "Hybrid beamforming for 5G and beyond millimeter-wave systems: A holistic view," *IEEE Open J. Commun. Soc.*, vol. 1, pp. 77–91, Dec. 2020.
- [20] W. Hong *et al.*, "The role of millimeter-wave technologies in 5G/6G wireless communications," *IEEE J. Microwaves*, vol. 1, no. 1, pp. 101–122, Jan. 2021.
- [21] A. Mahanfar, J. R. D. Luis, N. Apaydin, E. Yetisir, and S. K. Arani, "Antenna aperture in phased array antenna systems," U.S. Patent 0252801, Aug. 2019.
- [22] E. Degirmenci, "EMF test report: Ericsson AIR 5121," Ericsson AB, Stockholm, Sweden, Tech. Rep. GFTB-17:001589 Uen Rev B., Jan. 2018.
- [23] K. Kibaroglu, M. Sayginer, T. Phelps, and G. M. Rebeiz, "A 64-element 28-GHz phased-array transceiver with 52-dBm EIRP and 8-12-Gb/s 5G link at 300 meters without any calibration," *IEEE Trans. Microw. Theory Techn.*, vol. 66, no. 12, pp. 5796–5811, Dec. 2018.
- [24] B. Sadhu *et al.*, "A 28GHz 32-element phased-array transceiver IC with concurrent dual polarized beams and 1.4 degree beam-steering resolution for 5G communication," in *Proc. IEEE Int. Solid-State Circuits Conf.*, San Francisco, CA, USA, Feb. 2017, pp. 128–129.
- [25] R. Valkonen, "Compact 28-GHz phased array antenna for 5G access," in *IEEE MTT-S Int. Microw. Symp. Dig.*, Philadelphia, PA, USA, Jun. 2018, pp. 1334–1337.
- [26] Y. Aslan, C. E. Kiper, A. J. van den Biggelaar, U. Johannsen, and A. Yarovoy, "Passive cooling of mm-wave active integrated 5G base station antennas using CPU heatsinks," in *Proc. 16th Eur. Radar Conf.*, Paris, France, Oct. 2019, pp. 121–124.
- [27] J. Dunworth *et al.*, "A 28GHz phased array transceiver in 28 nm bulk CMOS for 5G prototype user equipment and base stations," in *Proc. IEEE/MTT-S Int. Microw. Symp. (IMS)*, Philadelphia, PA, USA, Jun. 2018, pp. 1330–1333.
- [28] H. Mohammadnezhad, R. Abedi, and P. Heydari, "A millimeter-wave partially overlapped beamforming-MIMO receiver: Theory, design, and implementation," *IEEE Trans. Microw. Theory Techn.*, vol. 67, no. 5, pp. 1924–1936, May 2019.
- [29] S. Mondal and J. Paramesh, "A reconfigurable 28-/37-GHz MMSE-adaptive hybrid-beamforming receiver for carrier aggregation and multi-standard MIMO communication," *IEEE J. Solid-State Circuits*, vol. 54, no. 5, pp. 1391–1406, May 2019.
- [30] S. Mondal, R. Singh, A. I. Hussein, and J. Paramesh, "A 25-30GHz fully-connected hybrid beamforming receiver for MIMO communication," *IEEE J. Solid-State Circuits*, vol. 53, no. 5, pp. 1275–1287, May 2018.
- [31] T. Kuwabara, N. Tawa, Y. Tone, and T. Kaneko, "A 28GHz 480 elements digital AAS using GaN HEMT amplifiers with 68 dBm EIRP for 5G long-range base station applications," in *Proc. IEEE Compound Semicond. Integr. Circuit Symp.*, Miami, FL, USA, Oct. 2017, pp. 1–4.
- [32] B. Yang, Z. Yu, J. Lan, R. Zhang, J. Zhou, and W. Hong, "Digital beamforming-based massive MIMO transceiver for 5G millimeter-wave communications," *IEEE Trans. Microw. Theory Techn.*, vol. 66, no. 7, pp. 3403–3418, May 2018.
- [33] W. Roh *et al.*, "Millimeter-wave beamforming as an enabling technology for 5G cellular communications: Theoretical feasibility and prototype results," *IEEE Commun. Mag.*, vol. 52, no. 2, pp. 106–113, Feb. 2014.
- [34] P. Xingdong, H. Wei, Y. Tianyang, and L. Linsheng, "Design and implementation of an active multibeam antenna system with 64 RF channels and 256 antenna elements for massive MIMO application in 5G wireless communications," *China Commun.*, vol. 11, no. 11, pp. 16–23, 2014.
- [35] U. Gustavsson *et al.*, "Implementation challenges and opportunities in beyond-5G and 6G communication," *IEEE J. Microwaves*, vol. 1, no. 1, pp. 86–100, Jan. 2021.
- [36] M. Schneider, C. Hartwanger, and H. Wolf, "Antennas for multiple spot beam satellites," *CEAS Space J.*, vol. 2, no. 1–4, pp. 59–66, Aug. 2011.
- [37] S. Rondineau *et al.*, "Ground stations of arrays to increase the LEO download capacity," in *Proc. IEEE Eur. Microw. Conf.*, Manchester, U.K., Sep. 2006, pp. 874–877.
- [38] G. Otto and J. Rhodes, "ThinKom unveils new multi-beam, reconfigurable, phased-array gateway solution for next-gen satellites," ThinKom PR, Hawthorne, CA, USA, Aug. 2019.
- [39] R. Gaudenzi, "Challenges in future satellite communications," in *Proc. IEEE Commun. Theory Workshop*, Miramar Beach, FL, USA, May 2018.
- [40] X. Song, T. Kühne, and G. Caire, "Fully-/partially-connected hybrid beamforming architectures for mmWave MU-MIMO," *IEEE Trans. Wireless Commun.*, vol. 19, no. 3, pp. 1754–1769, Mar. 2020.
- [41] M. S. Smith, *Introduction to Antennas*. Springer, London, U.K.: Macmillan, 1988.
- [42] J. Butler, "Beam-forming matrix simplifies design of electronically scanned antenna," *Electron. Des.*, vol. 9, pp. 170–173, 1961.
- [43] J. Blass, "Multidirectional antenna-a new approach to stacked beams," in *Proc. IRE Int. Conv. Rec.*, vol. 8, 1960, pp. 48–50.
- [44] H. Q. Ngo, *Massive MIMO: Fundamentals and System Designs*. LiU-Tryck, Linköping, Sweden: Linköping Univ. Electronic Press, 2015, vol. 1642.
- [45] Y. Aslan, S. Salman, J. Puskely, A. Roederer, and A. Yarovoy, "5G multi-user system simulations in line-of-sight with space-tapered cellular base station phased arrays," in *Proc. 13th Eur. Conf. Antennas Propag.*, Krakow, Poland, Apr. 2019, pp. 1–5.
- [46] Y. Aslan, A. Roederer, and A. Yarovoy, "System impacts of user scheduling with minimal angular separation constraints in radio resource management for 5G and beyond," in *Proc. IEEE Asia-Pacific Microw. Conf.*, Hong Kong, Dec. 2020, pp. 724–726.
- [47] H. Ren, Z. Zhang, Y. Jin, Y. Gu, and B. Arigong, "A novel 2D 3x3 Nolen matrix for 2D beamforming applications," *IEEE Trans. Microw. Theory Techn.*, vol. 67, no. 11, pp. 4622–4631, Nov. 2019.
- [48] M. A. B. Abbasi, H. Tataria, V. F. Fusco, and M. Matthaiou, "Performance of a 28GHz two-stage Rotman lens beamformer for millimeter wave cellular systems," in *Proc. 13th Eur. Conf. Antennas Propag.*, Krakow, Poland, Apr. 2019, pp. 1–4.
- [49] S. K. Berberian, *Introduction to Hilbert Space*. Providence, RI, USA: AMS, 1999, vol. 287.
- [50] R. J. Mailloux, *Phased Array Antenna Handbook*. London, U.K.: Artech House, 2017.
- [51] S. Foo, "Orthogonal-beam-space massive-MIMO array," in *Proc. IEEE APS Top. Conf. Antennas Propag. Wireless Commun.*, Turin, Italy, Sep. 2015, pp. 320–324.

- [52] J. Allen, "A theoretical limitation on the formation of lossless multiple beams in linear arrays," *IRE Trans. Antennas Propag.*, vol. 9, no. 4, pp. 350–352, Jul. 1961.
- [53] P. Angeletti, "Multiple beams from planar arrays," *IEEE Trans. Antennas Propag.*, vol. 62, no. 4, pp. 1750–1761, Apr. 2014.
- [54] S. P. Skobelev, "On the forming of orthogonal beams by planar array antennas," *IEEE Trans. Antennas Propag.*, vol. 62, no. 4, pp. 1762–1768, Jul. 2013.
- [55] S. Stein, "On cross coupling in multiple-beam antennas," *IRE Trans. Antennas Propag.*, vol. 10, no. 5, pp. 548–557, 1962.
- [56] J. S. Ajioka and H. A. Rosen, "Shaped beam antenna," U.S. Patent 3680143, Jul. 1972.
- [57] P. Angeletti and R. De Gaudenzi, "A pragmatic approach to massive MIMO for broadband communication satellites," *IEEE Access*, vol. 8, pp. 132 212–132 236, Jul. 2020.
- [58] J. Shelton and K. Kelleher, "Multiple beams from linear arrays," *IRE Trans. Antennas Propag.*, vol. 9, no. 2, pp. 154–161, 1961.
- [59] N. J. G. Fonseca, "Discussion on reciprocity, unitary matrix, and lossless multiple beam forming networks," *Int. J. Antennas Propag.*, vol. 2015, pp. 1–9, Apr. 2015.
- [60] S. Mosca, F. Bilotti, A. Toscano, and L. Vegni, "A novel design method for Blass matrix beam-forming networks," *IEEE Trans. Antennas Propag.*, vol. 50, no. 2, pp. 225–232, Feb. 2002.
- [61] W. C. Cummings, "Multiple beam forming networks," Massachusetts Inst. Tech. Lexington Lincoln Lab., Tech. Rep., 1978.
- [62] B. Piovano, L. Accatino, A. Angelucci, T. Jones, P. Capece, and M. Votta, "Design and breadboarding of wideband  $N \times N$  Butler matrices for multiport amplifiers," in *Proc. SBMO Int. Microw. Conf.*, vol. 1, Brazil, 1993, pp. 175–180.
- [63] T. A. Denidni and T. E. Libar, "Wide band four-port Butler matrix for switched multibeam antenna arrays," in *Proc. 14th IEEE Proc. Pers., Indoor Mobile Radio Commun.*, vol. 3, Beijing, China, Sep. 2003, pp. 2461–2464.
- [64] A. Tajik, M. Fakhrazadeh, and K. Mehrany, "DC to 40-GHz compact single-layer crossover," *IEEE Microw. Wireless Compon. Lett.*, vol. 28, no. 8, pp. 642–644, Jun. 2018.
- [65] L. Bustamante, G. Crone, N. Hill, A. Nubla, and J. Montero, " $8 \times 8$  Butler high power matrix at L-band," in *Proc. 25th Eur. Microw. Conf.*, vol. 2, Bologna, Italy, Sep. 1995, pp. 1046–1050.
- [66] M. Koubeissi, C. Decroze, T. Monediere, and B. Jecko, "Switched-beam antenna based on novel design of Butler matrices with broadside beam," *Electron. Lett.*, vol. 41, no. 20, pp. 1097–1098, 2005.
- [67] B. Wu, " $3 \times 3$  Butler matrix and  $5 \times 6$  Butler matrix," U.S. Pat. 9941587, Apr. 2018.
- [68] S. Odrobina, K. Staszek, K. Wincza, and S. Gruszczynski, "Broadband  $3 \times 3$  Butler matrix," in *Proc. IEEE Conf. Microw. Techn.*, Brno, Czech Republic, Apr. 2017, pp. 1–5.
- [69] G. Zhang, B.-H. Sun, L. Sun, J.-P. Zhao, Y. Geng, and R. Lian, "Design and implementation of a  $3 \times 3$  orthogonal beam-forming network for pattern-diversity applications," *Progr. Electromagn. Res.*, vol. 53, pp. 19–26, Aug. 2014.
- [70] A. Roederer and M. Martin, "Microwave hybrid coupler having  $3 \times n$  inputs and  $3 \times m$  outputs," U.S. Patent 5237294, Aug. 1993.
- [71] G. E. Evans, "Orthogonal beam forming network," U.S. Patent 4,638, 317, Jan. 1987.
- [72] K. Wu, M. Bozzi, and N. J. G. Fonseca, "Substrate integrated transmission lines: Review and applications," *IEEE J. Microwaves*, vol. 1, no. 1, pp. 345–363, Jan. 2021.
- [73] T. Djerafi and K. Wu, "A low-cost wideband 77GHz planar Butler matrix in SIW technology," *IEEE Trans. Antennas Propag.*, vol. 60, no. 10, pp. 4949–4954, Oct. 2012.
- [74] A. A. M. Ali, N. Fonseca, F. Coccetti, and H. Aubert, "Design and implementation of two-layer compact wideband Butler matrices in SIW technology for Ku-band applications," *IEEE Trans. Antennas Propag.*, vol. 59, no. 2, pp. 503–512, Feb. 2010.
- [75] W. Chen, Y. Hsieh, C. Tsai, Y. Chen, C. Chang, and S. Chang, "A compact two-dimensional phased array using grounded coplanar-waveguides Butler matrices," in *Proc. 9th Eur. Radar Conf.*, Amsterdam, The Netherlands, Nov. 2012, pp. 421–424.
- [76] J. Lian, Y. Ban, Q. Yang, B. Fu, Z. Yu, and L. Sun, "Planar millimeter-wave 2-D beam-scanning multibeam array antenna fed by compact SIW beam-forming network," *IEEE Trans. Antennas Propag.*, vol. 66, no. 3, pp. 1299–1310, Mar. 2018.
- [77] D. Kim, J. Hirokawa, and M. Ando, "Design of waveguide short-slot two-plane couplers for one-body 2-D beam-switching Butler matrix application," *IEEE Trans. Microw. Theory Techn.*, vol. 64, no. 3, pp. 776–784, Mar. 2016.
- [78] T. Tomura, D. Kim, M. Wakasa, Y. Sunaguchi, J. Hirokawa, and K. Nishimori, "A 20-GHz-band  $64 \times 64$  hollow waveguide two-dimensional Butler matrix," *IEEE Access*, vol. 7, pp. 164 080–164 088, Nov. 2019.
- [79] N. J. G. Fonseca, S. A. Gomanne, P. Castillo-Tapia, O. Quevedo-Teruel, T. Tomura, and J. Hirokawa, "Connecting networks for 2D Butler matrices generating a triangular lattice of beams," *IEEE J. Microwaves*, vol. 1, no. 2, pp. 646–658, Apr. 2021.
- [80] J. Nolen, "Synthesis of multiple beam networks for arbitrary illuminations," Ph.D. dissertation, Bendix Corp., Radio Division, Baltimore, MD, USA, Apr. 1965.
- [81] N. J. Fonseca, "Printed S-band 4 Nolen matrix for multiple beam antenna applications," *IEEE Trans. Antennas Propag.*, vol. 57, no. 6, pp. 1673–1678, Jun. 2009.
- [82] N. Fonseca, A. Ali, and H. Aubert, "Cancellation of beam squint with frequency in serial beamforming network-fed linear array antennas," *IEEE Antennas Propag. Mag.*, vol. 54, no. 1, pp. 32–39, Feb. 2012.
- [83] T. Djerafi, N. Fonseca, and K. Wu, "Planar Ku-band  $4 \times 4$  Nolen matrix in SIW technology," *IEEE Trans. Microw. Theory Techn.*, vol. 58, no. 2, pp. 259–266, Jan. 2010.
- [84] T. Djerafi, N. J. Fonseca, and K. Wu, "Broadband substrate integrated waveguide 4 Nolen matrix based on coupler delay compensation," *IEEE Trans. Microw. Theory Techn.*, vol. 59, no. 7, pp. 1740–1745, Jul. 2011.
- [85] J. Hirokawa and N. J. G. Fonseca, "Generalized one-dimensional parallel switching matrices with an arbitrary number of beams," *IEEE J. Microwaves*, vol. 1, no. 4, Oct. 2021, doi: 10.1109/JMW.2021.3106871.
- [86] H. Ren, H. Zhang, and B. Arigong, "Ultra-compact  $3 \times 3$  Nolen matrix beamforming network," *IET Microw. Antennas Propag.*, vol. 14, no. 3, pp. 143–148, Jan. 2020.
- [87] K. Wincza, S. Gruszczynski, and K. Sachse, "Reduced sidelobe four-beam antenna array fed by modified Butler matrix," *Electron. Lett.*, vol. 42, no. 9, pp. 508–509, Apr. 2006.
- [88] N. J. Fonseca and N. Ferrando, "Nolen matrix with tapered amplitude law for linear arrays with reduced side lobe level," in *Proc. 4th Eur. Conf. Antennas Propag.*, Barcelona, Spain, Apr. 2010, pp. 1–5.
- [89] J. G. K. J. Park, "A 28GHz CMOS Butler matrix for 5G mm-wave beamforming systems," *Microw. Opt. Technol. Lett.*, vol. 62, no. 7, pp. 2499–2505, Jul. 2020.
- [90] A. Tork and A. Natarajan, "Reconfigurable X-Band  $4 \times 4$  Butler array in 32 nm CMOS SOI for angle-reject arrays," in *Proc. IEEE/MTT-S Int. Microw. Symp.*, San Francisco, CA, USA, May 2016, pp. 1–3.
- [91] T.-Y. Chin, S.-F. Chang, C.-C. Chang, and J.-C. Wu, "A 24-GHz CMOS Butler matrix MMIC for multi-beam smart antenna systems," in *Proc. IEEE Radio Freq. Integr. Circuits Symp.*, Atlanta, GA, USA, Jun. 2008, pp. 633–636.
- [92] Y. Hu and W. Hong, "A novel hybrid analog-digital multibeam antenna array for massive MIMO applications," in *Proc. IEEE Asia Pacific Conf. Antennas Propag.*, Auckland, New Zealand, Aug. 2018, pp. 42–45.
- [93] R. Walter, "Multiple beam radar antenna system," U.S. Patent 3170158, Feb. 1965.
- [94] W. Rotman and R. Turner, "Wide-angle microwave lens for line source applications," *IEEE Trans. Antennas Propag.*, vol. 11, no. 6, pp. 623–632, Nov. 1963.
- [95] S. Vashist, M. Soni, and P. Singhal, "A review on the development of Rotman lens antenna," *Chin. J. Eng.*, vol. 2014, no. 11, pp. 1–9, Jul. 2014.
- [96] W. White, "Pattern limitations in multiple-beam antennas," *IRE Trans. Antennas Propag.*, vol. 10, no. 4, pp. 430–436, 1962.
- [97] M. Smith, "Multiple beam crossovers for a lens-fed antenna array," *Radio Electron. Eng.*, vol. 55, no. 1, pp. 33–36, 1985.
- [98] M. B. Shemirani and F. Aryanfar, "Analog implementation of high resolution DFT in RF domain, utilizing a special multilayer realization of Rotman lens," in *Proc. IEEE Antennas Propag. Soc. Int. Symp.*, San Diego, CA, USA, Jul. 2008, pp. 1–4.

- [99] Y. Zhang and V. Fusco, "Fourier transform using a Rotman lens," in *Proc. 9th Eur. Radar Conf.*, Amsterdam, The Netherlands, Nov. 2012, pp. 389–392.
- [100] H.-T. Chou, S.-J. Chou, C.-W. Chiu, C.-C. Sun, and C.-T. Yu, "Quasi-orthogonal multibeam radiation of reflector antennas for radio coverage of mobile communication at millimeter-wave frequencies," *IEEE Trans. Antennas Propag.*, vol. 66, no. 11, pp. 6340–6345, Aug. 2018.
- [101] J. G.-G. Trujillo, Á. N. S. de Toca, I. M. Ortego, J. M. F. González, and M. S. Pérez, "Design and implementation of a quasi-orthogonal switching beam-former for triangular arrays of three radiating elements," *IEEE Trans. Antennas Propag.*, vol. 61, no. 10, pp. 5028–5035, Oct. 2013.
- [102] S. Foo, "Orthogonal-beam-space spatial multiplexing radio communication system and associated antenna array," U.S. Patent 10158173, Dec. 2018.
- [103] H. Ren, B. Arigong, M. Zhou, J. Ding, and H. Zhang, "A novel design of 4×4 butler matrix with relatively flexible phase differences," *IEEE Antennas Wireless Propag. Lett.*, vol. 15, pp. 1277–1280, Jan. 2015.
- [104] H. Liu, S. Fang, Z. Wang, and S. Fu, "Design of arbitrary-phase-difference transdirectional coupler and its application to a flexible butler matrix," *IEEE Trans. Microw. Theory Techn.*, vol. 67, no. 10, pp. 4175–4185, Aug. 2019.
- [105] S. Golabighezlahmad, E. Klumperink, and B. Nauta, "A 1-4 GHz 4×4 MIMO receiver with 4 reconfigurable orthogonal beams for analog interference rejection," in *Proc. IEEE Radio Freq. Integr. Circuits Symp.*, Boston, MA, USA, Jun. 2019, pp. 339–342.
- [106] D. C. Chang, "Interference rejections of satellite ground terminal with orthogonal beams," U.S. Patent 13904051, Dec. 2013.
- [107] P. Wongchampa and M. Uthansakul, "Orthogonal beamforming for multiuser wireless communications: Achieving higher received signal strength and throughput than with conventional beamforming," *IEEE Antennas Propag. Mag.*, vol. 59, no. 4, pp. 38–49, Jun. 2017.
- [108] P. Wongchampa, "Reduction of interference using orthogonal vertical beamforming in an indoor communication," in *Proc. MATEC Web Conf.*, vol. 277, Apr. 2019, pp. 1–6.
- [109] S. Jain, Y. Wang, and A. Natarajan, "A 10GHz CMOS RX frontend with spatial cancellation of co-channel interferers for MIMO/digital beamforming arrays," in *Proc. IEEE Radio Freq. Integr. Circuits Symp.*, San Francisco, CA, USA, May 2016, pp. 99–102.
- [110] L. Zhang and H. Krishnaswamy, "A 0.1-to-3.1GHz 4-element MIMO receiver array supporting analog/RF arbitrary spatial filtering," in *Proc. IEEE Int. Solid-State Circuits Conf.*, San Francisco, CA, USA, Feb. 2017, pp. 410–411.
- [111] L. Zhang, A. Natarajan, and H. Krishnaswamy, "A scalable 0.1-to-1.7GHz spatio-spectral-filtering 4-element MIMO receiver array with spatial notch suppression enabling digital beamforming," in *Proc. IEEE Int. Solid-State Circuits Conf.*, San Francisco, CA, USA, Feb. 2016, pp. 166–167.
- [112] S. Spira, K. Blau, R. Thomä, and M. A. Hein, "Agile multi-beam front-end for 5G mm-wave measurements," *Int. J. Microw. Wireless Technol.*, vol. 13, pp. 740–750, 2021.
- [113] D.-C. Kim, S.-J. Park, T.-W. Kim, L. Minz, and S.-O. Park, "Fully digital beamforming receiver with a real-time calibration for 5G mobile communication," *IEEE Trans. Antennas Propag.*, vol. 67, no. 6, pp. 3809–3819, Jun. 2019.
- [114] B. Sadhu *et al.*, "A 28-GHz 32-element TRX phased-array IC with concurrent dual-polarized operation and orthogonal phase and gain control for 5G communications," *IEEE J. Solid-State Circuits*, vol. 52, no. 12, pp. 3373–3391, Dec. 2017.
- [115] H.-T. Kim *et al.*, "A 28-GHz CMOS direct conversion transceiver with packaged 2×4 antenna array for 5G cellular system," *IEEE J. Solid-State Circuits*, vol. 53, no. 5, pp. 1245–1259, May 2018.
- [116] J. D. Dunworth *et al.*, "A 28GHz bulk-CMOS dual-polarization phased-array transceiver with 24 channels for 5G user and basestation equipment," in *Proc. IEEE Int. Solid-State Circuits Conf.*, San Francisco, CA, USA, Feb. 2018, pp. 70–72.
- [117] M. Sharif and B. Hassibi, "On the capacity of MIMO broadcast channels with partial side information," *IEEE Trans. Inf. Theory*, vol. 51, no. 2, pp. 506–522, Jan. 2005.
- [118] J. L. Vicario, R. Bosio, C. Anton-Haro, and U. Spagnolini, "Beam selection strategies for orthogonal random beamforming in sparse networks," *IEEE Trans. Wireless Commun.*, vol. 7, no. 9, pp. 3385–3396, Sep. 2008.
- [119] D.-C. Oh and Y.-H. Lee, "Multi-user diversity and multiplexing with orthogonal multiple beams in packet-based wireless systems," *Eur. Trans. Telecommun.*, vol. 21, no. 3, pp. 288–297, Apr. 2010.
- [120] R. De Francisco, M. Kountouris, D. T. Slock, and D. Gesbert, "Orthogonal linear beamforming in MIMO broadcast channels," in *Proc. IEEE Wireless. Commun. Netw. Conf.*, Hong Kong, China, Mar. 2007, pp. 1210–1215.
- [121] K. Matsumura and T. Ohtsuki, "Orthogonal beamforming using Gram-Schmidt orthogonalization for multi-user MIMO downlink system," *EURASIP J. Wireless Commun. Netw.*, vol. 2011, no. 1, pp. 1–10, Jul. 2011.
- [122] Y. Na and H. Jin, "Orthogonal/partial orthogonal beamforming weight generation for MIMO wireless communication," U.S. Patent 7884763, Feb. 2011.
- [123] K. Huang, J. G. Andrews, and R. W. Heath, "Performance of orthogonal beamforming for SDMA with limited feedback," *IEEE Trans. Veh. Technol.*, vol. 58, no. 1, pp. 152–164, May 2008.
- [124] C. Simon and G. Leus, "Round-robin scheduling for orthogonal beamforming with limited feedback," *IEEE Trans. Wireless Commun.*, vol. 10, no. 8, pp. 2486–2496, Jun. 2011.
- [125] F. Fakoukakis, S. Diamantis, A. Orfanides, and G. Kyriacou, "Development of an adaptive and a switched beam smart antenna system for wireless communications," *J. Electromagn. Waves Appl.*, vol. 20, no. 3, pp. 399–408, 2006.
- [126] B. Allen and M. Beach, "On the analysis of switched-beam antennas for the W-CDMA downlink," *IEEE Trans. Veh. Technol.*, vol. 53, no. 3, pp. 569–578, May 2004.
- [127] J. Brady and A. Sayeed, "Beamspace MU-MIMO for high-density gigabit small cell access at millimeter-wave frequencies," in *Proc. IEEE 15th Int. Workshop Signal Process. Adv. Wireless Commun.*, Toronto, ON, Canada, Jun. 2014, pp. 80–84.
- [128] J. Wang, H. Zhu, L. Dai, N. J. Gomes, and J. Wang, "Low-complexity beam allocation for switched-beam based multiuser massive MIMO systems," *IEEE Trans. Wireless Commun.*, vol. 15, no. 12, pp. 8236–8248, Dec. 2016.
- [129] A. Roederer, "Multibeam antenna feed device," U.S. Patent 5115248, May 1992.
- [130] C.-H. H. Chen, B. R. Allen, K. T. Yano, M. Kintis, and S. S. Kuo, "Enhanced direct radiating array," U.S. Patent 6295026, Sep. 2001.
- [131] D. Petrolati, P. Angeletti, and G. Toso, "A lossless beam-forming network for linear arrays based on overlapped sub-arrays," *IEEE Trans. Antennas Propag.*, vol. 62, no. 4, pp. 1769–1778, Sep. 2013.
- [132] P. Angeletti, "Reconfigurable beam-forming-network architecture," U.S. Patent 8451172, May 2013.
- [133] W.-L. Hung, C.-H. Chen, C.-C. Liao, C.-R. Tsai, and A.-Y. A. Wu, "Low-complexity hybrid precoding algorithm based on orthogonal beamforming codebook," in *Proc. IEEE Workshop Signal Process. Syst.*, Hangzhou, China, Oct. 2015, pp. 1–5.
- [134] J. Wang, H. Zhu, N. J. Gomes, and J. Wang, "Frequency reuse of beam allocation for multiuser massive MIMO systems," *IEEE Trans. Wireless Commun.*, vol. 17, no. 4, pp. 2346–2359, Jan. 2018.
- [135] A. Ghasemi and S. A. Zekavat, "Low-cost mmWave MIMO multi-streaming via bi-clustering, graph coloring, and hybrid beamforming," *IEEE Trans. Wireless Commun.*, vol. 20, no. 7, pp. 4113–4127, Jul. 2021.
- [136] J. Zhang, W. Liu, C. Gu, S. S. Gao, and Q. Luo, "Multi-beam multiplexing design for arbitrary directions based on the interleaved subarray architecture," *IEEE Trans. Veh. Technol.*, vol. 69, no. 10, pp. 11 220–11 232, Oct. 2020.
- [137] V. T. Campana, H.-G. Yeh, J. Lee, and D. Chang, "Multiple orthogonal beams with multi-user and frequency reuse via active scattering devices," in *Proc. Annu. IEEE Syst. Conf.*, Orlando, FL, USA, Jun. 2016, pp. 1–6.
- [138] J. Montesinos, O. Besson, and C. L. De Tournemine, "Adaptive beamforming for large arrays in satellite communications systems with dispersed coverage," *IET Commun.*, vol. 5, no. 3, pp. 350–361, Feb. 2011.
- [139] Y. Aslan, J. Puskely, A. Roederer, and A. Yarovoy, "Trade-offs between the quality of service, computational cost and cooling complexity in interference-dominated multi-user SDMA systems," *IET Commun.*, vol. 14, no. 1, pp. 144–151, Jan. 2020.
- [140] C.-S. Park, Y.-S. Byun, A. M. Bokiye, and Y.-H. Lee, "Complexity reduced zero-forcing beamforming in massive MIMO systems," in *Proc. IEEE Inf. Theory Appl. Workshop*, San Diego, CA, USA, Feb. 2014, pp. 1–5.

- [141] C. Zhang, W. Xu, and M. Chen, "Hybrid zero-forcing beamforming/orthogonal beamforming with user selection for MIMO broadcast channels," *IEEE Commun. Lett.*, vol. 13, no. 1, pp. 10–12, Jan. 2009.
- [142] S. K. Yong, M. E. Sahin, and Y. H. Kim, "On the effects of misalignment and angular spread on the beamforming performance," in *Proc. IEEE CCCN*, 2007, pp. 1–5.
- [143] S. Saur, H. Halbauer, A. Rueegg, and F. Schaich, "Grid-of-beams (GoB) based downlink multi-user MIMO," *IEEE 802.16 Broadband Wireless Access Work. Group Std.*, vol. 802, pp. 1–4, May 2008.
- [144] J. Tan et al., "Random access channel with a grid of beams for communication systems," U.S. Patent App. 14524726, Apr. 2016.
- [145] R. S. Ganesan, W. Zirwas, B. Panzner, K. I. Pedersen, and K. Valkealahti, "Integrating 3D channel model and grid of beams for 5G mMIMO system level simulations," in *Proc. IEEE 84th Veh. Technol. Conf.*, Montreal, QC, Canada, Sep. 2016, pp. 1–6.
- [146] M. Thurfjell, A. Simonsson, O. Lundberg, and O. Rosin, "Narrow beam channel characteristics measured on an 5G NR grid-of-beam test-bed," in *Proc. IEEE 87th Veh. Technol. Conf.*, Porto, Portugal, Jun. 2018, pp. 1–4.
- [147] A. F. Morabito, T. Isernia, M. G. Labate, M. Durso, and O. M. Bucci, "Direct radiating arrays for satellite communications via aperiodic tilings," *Progr. Electromagn. Res.*, vol. 93, pp. 107–124, 2009.
- [148] O. Bucci, T. Isernia, A. Morabito, S. Perna, and D. Pinchera, "Aperiodic arrays for space applications: An effective strategy for the overall design," in *Proc. 3rd IEEE Eur. Conf. Antennas Propag.*, Berlin, Germany, Mar. 2009, pp. 2031–2035.
- [149] A. Catalani, L. Russo, O. Bucci, T. Isernia, G. Toso, and P. Angeletti, "Ka-band active sparse arrays for satcom applications," in *Proc. IEEE Int. Symp. Antennas Propag.*, Chicago, IL, USA, Jul. 2012, pp. 1–2.
- [150] C. Bencivenni, M. Ivashina, R. Maaskant, and J. Wettergren, "Synthesis of maximally sparse arrays using compressive sensing and full-wave analysis for global earth coverage applications," *IEEE Trans. Antennas Propag.*, vol. 64, no. 11, pp. 4872–4877, Jul. 2016.
- [151] D. Pinchera, M. D. Migliore, and G. Panariello, "Synthesis of large sparse arrays using IDEA (inflating-deflating exploration algorithm)," *IEEE Trans. Antennas Propag.*, vol. 66, no. 9, pp. 4658–4668, Jun. 2018.
- [152] O. M. Bucci, M. D'Urso, T. Isernia, P. Angeletti, and G. Toso, "Deterministic synthesis of uniform amplitude sparse arrays via new density taper techniques," *IEEE Trans. Antennas Propag.*, vol. 58, no. 6, pp. 1949–1958, Mar. 2010.
- [153] M. C. Viganó, G. Toso, G. Caille, C. Mangenot, and I. E. Lager, "Sunflower array antenna with adjustable density taper," *Int. J. Antennas Propag.*, vol. 2009, pp. 1–10, Apr. 2009.
- [154] Y. Aslan, J. Puskely, A. Roederer, and A. Yarovoy, "Multiple beam synthesis of passively cooled 5G planar arrays using convex optimization," *IEEE Trans. Antennas Propag.*, vol. 68, no. 5, pp. 3557–3566, Dec. 2019.
- [155] Y. Aslan, A. Roederer, and A. G. Yarovoy, "Synthesis of optimal 5G array layouts with wide-angle scanning and zooming ability for efficient link setup and high-QoS communication," *IEEE Antennas Wireless Propag. Lett.*, vol. 19, no. 9, pp. 1481–1485, Sep. 2020.
- [156] X. Ge, R. Zi, H. Wang, J. Zhang, and M. Jo, "Multi-user massive MIMO communication systems based on irregular antenna arrays," *IEEE Trans. Wireless Commun.*, vol. 15, no. 8, pp. 5287–5301, Apr. 2016.
- [157] C. Bencivenni, M. Coldrey, R. Maaskant, and M. Ivashina, "Aperiodic switched array for line-of-sight MIMO backhauling," *IEEE Antennas Wireless Propag. Lett.*, vol. 17, no. 9, pp. 1712–1716, Sep. 2018.
- [158] C. Bencivenni, A. A. Glazunov, R. Maaskant, and M. V. Ivashina, "Effects of regular and aperiodic array layout in multi-user MIMO applications," in *Proc. IEEE Int. Symp. Antennas Propag. USNC/URSI Nat. Radio Sci. Meeting*, San Diego, CA, USA, Jul. 2017, pp. 1877–1878.
- [159] N. Amani, R. Maaskant, and W. Van Cappellen, "On the sparsity and aperiodicity of a base station antenna array in a downlink MU-MIMO scenario," in *Proc. IEEE Int. Symp. Antennas Propag.*, Busan, South Korea, Oct. 2018, pp. 1–2.
- [160] N. Amani, C. Bencivenni, A. A. Glazunov, M. V. Ivashina, and R. Maaskant, "MIMO channel capacity gains in mm-wave los systems with irregular sparse array antennas," in *Proc. IEEE APS Top. Conf. Antennas Propag. Wireless Commun.*, Verona, Italy, Sep. 2017, pp. 264–265.
- [161] Y. Aslan, J. Puskely, J. Janssen, M. Geurts, A. Roederer, and A. Yarovoy, "Thermal-aware synthesis of 5G base station antenna arrays: An overview and a sparsity-based approach," *IEEE Access*, vol. 6, pp. 58 868–58 882, Oct. 2018.
- [162] Y. Aslan, J. Puskely, A. Roederer, and A. Yarovoy, "Effect of element number reduction on inter-user interference and chip temperatures in passively-cooled integrated antenna arrays for 5G," in *Proc. 14th Eur. Conf. Antennas Propag.*, Copenhagen, Denmark, Mar. 2020, pp. 1–5.
- [163] Y. Aslan, A. Roederer, and A. Yarovoy, "System advantages of using large scale aperiodic array topologies in future mm-wave 5G/6G base stations: An interdisciplinary look," *IEEE Syst. J.*, early access, Jan. 11, 2021, doi: [10.1109/JSYST.2020.3045909](https://doi.org/10.1109/JSYST.2020.3045909).



**YANKI ASLAN** (Member, IEEE) was born in Ankara, Turkey, in 1991. He received the B.Sc. degree with double specialization in communications and microwaves/antennas from the Department of Electrical and Electronic Engineering, Middle East Technical University, Ankara, Turkey, in 2014, and the M.Sc. (*cum laude*) and Ph.D. degrees (*cum laude*) in electrical engineering from Delft University of Technology, Delft, The Netherlands, in 2016 and 2020, respectively. Following his Postdoctoral Research with Delft University of Technology in the Microwave Sensing, Signals and Systems (MS3) Group, he was an Assistant Professor with TU Delft in April 2021. His current research interests include phased arrays for next-generation communication and sensing systems, array optimization, multibeam antennas, front-end architectures, and beamforming algorithms. Dr. Aslan was one of the recipients of the IEEE AP-S Doctoral Research Grant in 2018 and the EuMA Internship Award in 2019. He was the recipient of the Justus & Louise van Effen Scholarship from Delft University of Technology for his M.Sc. degree.



**ANTOINE ROEDERER** (Life Fellow, IEEE) was born in Paris in 1943. He received the B.S.E.E. degree from the l'Ecole Supérieure d'Electricité, Paris, France, in 1964, the M.S.E.E. degree from the University of California at Berkeley, Berkeley, CA, USA, in 1965, the Doctorate degree (Hons.) in electrical engineering from the Université de Paris VI, Paris, in 1972, and the Honorary Doctorate degree from the Technical University of Delft, Delft, The Netherlands, in 2005.

From 1968 to 1973, he was a Radar Antenna R&D Engineer with THOMSON-CSF, Bagnoux, France. In 1973, he joined European Space Research and Technology Centre, ESRO (now ESA, the European Space Agency), Noordwijk, The Netherlands, where he initiated and supervised for many years research and development and project support for space antennas. In 1993, he became the Head of Electromagnetics Division, ESA. He is currently a part-time Scientific Advisor with the Technical University of Delft. He has authored or coauthored more than 150 articles, several book chapters, and holds 20 patents in the field of antennas. This has included aspects of wideband communications, broadcasting, radar, and satellite antennas, with an emphasis on log-periodics, reflectarrays, multiple-beam reflectors and arrays, and advanced antenna feed networks. His current research interests include innovation and development in the fields of radar and 5G base station antennas.

Dr. Roederer was the recipient of numerous awards for his contributions to the field of antennas and to the antenna community in Europe. He was the recipient of the Fulbright Fellowship for his M.S.E.E. degree. He has been the Chairman of the EU COST 260 Project on Smart Antennas. He was the Initiator and the Chairman of the Millennium Conference on Antennas and Propagation (AP 2000), Davos, precursor of the large EUCAP conferences. He retired from ESA in 2008.



**NELSON J. G. FONSECA** (Senior Member, IEEE) received the M.Eng. degree in electrical engineering and signal processing from Ecole Nationale Supérieure d'Electrotechnique, Electronique, Informatique, Hydraulique et Télécommunications (ENSEEIH), Toulouse, France, in 2003, the M.Sc. degree in electrical engineering from the Ecole Polytechnique de Montreal, QC, Canada, in 2003, and the Ph.D. degree in electrical engineering from the Institut National Polytechnique de Toulouse – Université de Toulouse, France, in

2010.

He is currently an Antenna Engineer for the Antenna and Sub-Millimeter Waves Section, European Space Agency (ESA), Noordwijk, The Netherlands. Since November 2020, he holds an Honorary Appointment as Professional Fellow with the University of Technology Sydney, Sydney, NSW, Australia. He has authored or coauthored more than 230 papers in peer-reviewed journals and conferences and has more than 50 patents issued or pending. His research interests include multiple beam antennas for space missions, beamformer theory and design, ground terminal antennas, transfer of technology from and to terrestrial systems, including 5G networks, and novel manufacturing techniques.

Dr. Fonseca was the Chair of the 38th ESA Antenna workshop in 2017, and the Co-Chair of the 2018 IET Loughborough Antennas & Propagation conference (LAPC 2018). He is currently an Associate Editor for *IET Microwaves, Antennas, and Propagation* (MAP) and IEEE TRANSACTIONS ON MICROWAVE THEORY AND TECHNIQUES (TMTT), and a Topic Editor of IEEE JOURNAL OF MICROWAVES (JM). He is also the Co-Vice Chair of the newly founded IEEE MTT-S Technical Committee 29 (MTT-29) on Microwave Aerospace Systems. He has been a Board Member of the European School of Antennas and Propagation (ESoA) since January 2019 and is also serving as the coordinator of the ESA/ESoA course on Antennas for Space Applications, for which he was voted best Lecturer by the participants of the 2020 edition. He is the elected EurAAP Regional Delegate representing Benelux for the term 2021–2023. He was the recipient of several prizes and awards, including the Best Young Engineer Paper Award at the 29th ESA Workshop on Antennas in 2007, the ESA Teamwork Excellence Award in 2020, and multiple ESA technical improvement awards.



**PIERO ANGELETTI** (Senior Member, IEEE) received the Laurea degree (summa cum laude) in electronics engineering from the University of Ancona, Italy, in 1996 and the Ph.D. degree in electromagnetism from the University of Rome La Sapienza, Italy, in 2010. He has more than 20 years of experience in RF systems engineering and technical management encompassing conceptual/architectural design, trade-offs, detailed design, production, integration and testing of satellite payloads, and active antenna systems for commercial/military telecommunications and navigation (spanning all the operating bands and set of applications) and also for multifunction RADARs and electronic counter measure systems. He has authored or coauthored more than 300 technical reports, book chapters, and articles published in peer reviewed professional journals and international conferences proceedings. He holds several patents related to satellite payload and antenna technology. He is currently a Member of the Technical Staff of the European Space Research and Technology Center (ESTEC), European Space Agency, Noordwijk, The Netherlands. He is heading the Radio Frequency Payloads and Technology Division, Directorate of Technology, Engineering and Quality (TEC), which is responsible for RF payloads, instruments, and relevant technologies. In particular, he oversees ESA research and development activities related to flexible satellite payloads, RF front-ends, and on-board digital processors. Together with Giovanni Toso, he is an instructor of the course on multibeam antennas and beamforming networks, which has been offered at main IEEE and European microwaves, wireless and antenna conferences, such as IEEE APS, IEEE IMS, EuMW, EuCAP, the IEEE ICWITS, and ESA Internal University, since 2012.

2010.



**ALEXANDER YAROVOY** (Fellow, IEEE) received the Diploma degree (Hons.) in radiophysics and electronics and the Candidate Phys. and Math. Sci. and Doctor Phys. and Math. Sci. degrees in radiophysics from Kharkov State University, Kharkiv, Ukraine, in 1984, 1987, and 1994, respectively.

In 1987, he joined the Department of Radiophysics, Kharkov State University, as a Researcher, where he became a Professor in 1997. From September 1994 to 1996, he was with the Technical University of Ilmenau, Ilmenau, Germany, as a

Visiting Researcher. Since 1999, he has been with Delft University of Technology, Delft, The Netherlands. Since 2009, he has been leading the Chair of Microwave Sensing, Systems and Signals. He has authored or coauthored more than 450 scientific or technical articles, four patents, and 14 book chapters. His main research interests include high-resolution radar, microwave imaging, and applied electromagnetics (in particular, UWB antennas).

Dr. Yarovoy was the recipient of the European Microwave Week Radar Award for the paper that best advances the state-of-the-art in radar technology in 2001 (together with L.P. Ligthart and P. van Genderen) and in 2012 (together with T. Savelyev). In 2010, together with D. Caratelli, he was the recipient of the Best Paper Award of the Applied Computational Electromagnetic Society (ACES). Prof. Yarovoy served as the General TPC chair of the 2020 European Microwave Week (EuMW'20), as the Chair and TPC chair of the 5th European Radar Conference (EuRAD'08), as well as the Secretary of the 1st European Radar Conference (EuRAD'04). He was also the Co-Chair and the TPC Chair of the 10th International Conference on GPR (GPR2004), Delft, The Netherlands. From 2008 to 2017, he was the Director of the European Microwave Association (EuMA). He was a Guest Editor of five special issues of IEEE TRANSACTIONS and other journals. From 2011 to 2018, he was an Associate Editor for *International Journal of Microwave and Wireless Technologies*.